2013-01-01

Assessment Of Abaqus Capabilities For Crack Growth And Calculation Of Energy Release Rate

Luis Alonso Hernandez
University of Texas at El Paso, lahernandez2@miners.utep.edu

ASSESSMENT OF ABAQUS CAPABILITIES FOR CRACK GROWTH AND CALCULATION OF ENERGY RELEASE RATE

LUIS A. HERNANDEZ

Department of Mechanical Engineering

APPROVED:

Jack F. Chessa, Ph.D., Chair

Yirong Lin, Ph.D.

Stephen W. Stafford, Ph.D.

Benjamin C. Flores, Ph.D.
Dean of the Graduate School

DEDICATION

I want to dedicate this work to my family, especially to Jorge Hernandez, Rosa Proa, Manuel Proa, Socorro Morales, Mely Proa, Samantha Dominguez, and Melissa Dominguez.

ASSESSMENT OF ABAQUS CAPABILITIES FOR CRACK GROWTH AND CALCULATION OF ENERGY RELEASE RATE

by

LUIS A. HERNANDEZ, B.S. ME

THESIS

Presented to the Faculty of the Graduate School of

The University of Texas at El Paso

in Partial Fulfillment

of the Requirements

for the Degree of

MASTER OF SCIENCE

Department of Mechanical Engineering

THE UNIVERSITY OF TEXAS AT EL PASO

AUGUST 2013

ACKNOWLEDGEMENTS

Special thanks to Dr. Chessa, who supported me and guided me through the process of becoming a conscientious student. Special thanks to Dr. Lin and Dr. Stafford who taught me the basics of fracture mechanics during the classes I took with them.

ABSTRACT

The purpose of this study was to benchmark ABAQUS modeling capabilities for crack propagation and calculation of energy release rate against closed-form analytical solutions. The crack growth capability for this study was evaluated using the following techniques: virtual crack closure technique (VCCT), X-FEM coupled with VCCT, and X-FEM coupled with cohesive segments. The capability of calculating the energy release rate was assessed by using the J-integral routine. A Double Cantilever Beam (DCB) specimen was used to conduct the study for mode I propagation, and a mixed mode bending (MMB) specimen was used to study the propagation for mixed mode I/II with a mixed mode ratio of $G_{II}/G_T=0.5$, both specimens were modeled using elastic properties. The contour integral analysis for energy release rate was done by modeling an edge crack in an infinite plate in tension. Results obtained for crack growth and energy release were in good agreement with the closed-from analytical solutions, load/displacement plots and contour integral results are presented. Overall, results are encouraging but further assessment for comparing ABAQUS against experimental results is strongly suggested.

TABLE OF CONTENTS

LIST OF TABLES

LIST OF FIGURES

1. INTRODUCTION

Fracture is a problem that society has faced for as long as there have been man-made structures. The problem may actually be worse today than in previous centuries, because more can go wrong in our complex technological society. Fortunately, advances in the field of fracture mechanics have helped to offset some of the potential dangers posed by increasing technological complexity [3]. This study was focused in a branch within fracture mechanics: computational fracture mechanics (CFM).

The role of computational fracture mechanics has been expanding. Not only does it continue to encompass its classic responsibility to compute driving forces, but it is now also frequently employed to predict a material's resistance to crack growth and even the process of nucleation itself [9]. In computational fracture mechanics there are several techniques that help the analyst to obtain stress intensity factors, energy release rates, simulate crack growth and solve specials problems: dynamic fracture, ductile fracture, and cohesive fracture among others. The goal of this study was to benchmark ABAQUS against closed-form analytical solutions for crack growth and calculation of energy release rate.

This thesis is organized as follows: literature review section, where concepts of linear elastic fracture mechanics, crack growth analysis methods, X-FEM concepts, and the J-integral are introduced; the methodology section provides the process used to benchmark ABAQUS, within this section, the used geometry, properties of the selected material, the set-up of the used techniques, and an explanation on how the parameters were selected is presented; the results section presents load/displacement relationships for crack growth in mode I and mixed mode I/II, and the results obtained for energy release rate by the J-integral. Finally, recommendations for future work are offered.

2. LITERATURE REVIEW

2.1 LINEAR ELASTIC FRACTURE MECHANICS

The concepts of fracture mechanics that were derived prior to 1960 are applicable only to materials that obey Hooke's law [3]. Linear elastic fracture mechanics (LEFM) assumes that the material is isotropic and linear elastic and when the stresses near the crack tip exceed the material fracture toughness, the crack will grow. The formulas used for LEFM are derived for either plane stress or plane strain, and are associated with the three basic modes of loadings in a cracked body, see figure 1. The formulas presented are: energy release rate and the relationship between energy release rate and stress intensity factor.

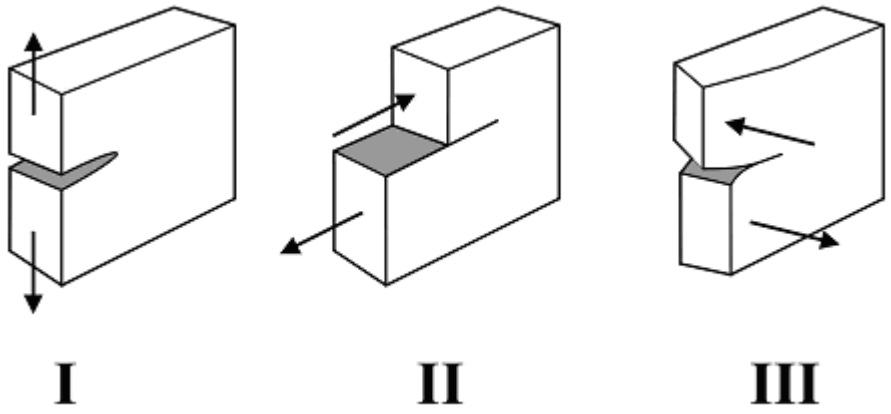

Fig. 1 The three modes of loading that can be applied to a crack

I) Opening mode

II) Sliding mode

III) Tearing mode

In 1956 Irwin proposed an energy approach for fracture, he defined an energy release rate, *G*, which is a measure of the energy available for an increment of crack extension [3].

The term rate refers to the change in potential energy with respect to area as seen in formula 1. The term *G* it is also called the crack extension force or crack driving force.

$$G = -\frac{d\Pi}{dA} \tag{1}$$

Crack growth may be stable or unstable, depending how G and fracture energy vary with crack size. Crack extension occurs when G=R, where R refers to the material resistance to crack extension. The conditions for stable crack growth can be expressed as follows:

$$G = R \tag{2}$$

and

$$\frac{dG}{da} \leq \frac{dR}{da} \tag{3}$$

Unstable crack growth occurs when

$$\frac{dG}{da} > \frac{dR}{da} \tag{4}$$

In other words, if the crack grows stable, more loading is needed to extend it, while if the growth is unstable, it will extend until it reaches complete fracture.

The stress intensity factor, denoted by letter K, is another important parameter that describes the behavior of cracks. The stress intensity factor is used in fracture mechanics to predict the stress state near the tip of a crack caused by a remote load or residual stresses [3]. The stress intensity factor is usually given a subscript to denote the mode of loading; i.e., K_{I}, K_{II}, or K_{III}. Now that both parameters have been introduced, we can make the following statement: the energy release rate, G, describes global behavior, while the stress intensity factor, K, is a local parameter. For linear elastic fracture mechanics, K and G are uniquely related.

For a crack in an infinite plate subject to a tensile stress, we can get the following relationship:

$$G = \frac{K_I^2}{E'} \tag{5}$$

where for plane stress conditions

$$E' = E \tag{6}$$

and for plane strain conditions

$$E' = \frac{E}{1-\nu^2} \tag{7}$$

where ν is the Poisson's ratio and E is the Young's Modulus for elasticity.

Another important topic to be discussed in this section is load control versus displacement control. As discussed before, crack growth stability depends on the rate of change of G, although the

driving force G is the same for both load control and displacement control, the rate of change of the driving force curve depends on how the structure is loaded. Displacement control tends to be more stable than load control; the reason is that with some configurations, the driving force actually decreases with crack growth in displacement control [3].

2.2 CRACK GROWTH MODELING TECHNNIQUES

The virtual crack closure technique (VCCT) and cohesive zone modeling (CZM) are some of the techniques used for crack modeling; X-FEM will be discussed in another subsection. Each of these two techniques must have its own crack growth criterion. The techniques and the crack growth criterion of each one will be introduced.

2.2.1 VCCT

The VCCT is widely used for computing energy release rates based on results from continuum (2D) and solid (3D) finite element analysis and to supply the mode separation required when used the mixed mode fracture criterion [3]. VCCT was originally proposed in 1977 by Rybicki and Kaninen [7], this paper explains that the crack closure method is based on Irwin's crack closure integral. In literature sometimes the VCCT is used with one or two steps, an explanation of both techniques will be explained as mentioned in [15].

The two-step VCCT method is based on the assumption that energy released when the crack is extended by Δa from a (figure 2) to $a + \Delta a$ (figure 3) is identical to close the crack between location ℓ to i. Index 1 in formula 8 denotes the first step and index 2 is the second step. For a two-step method the energy required goes as follows:

$$G_{equiv} = \frac{1}{2}[X_{1l} * \Delta u_{2l} + Z_{1l} * \Delta w_{2l}] \tag{8}$$

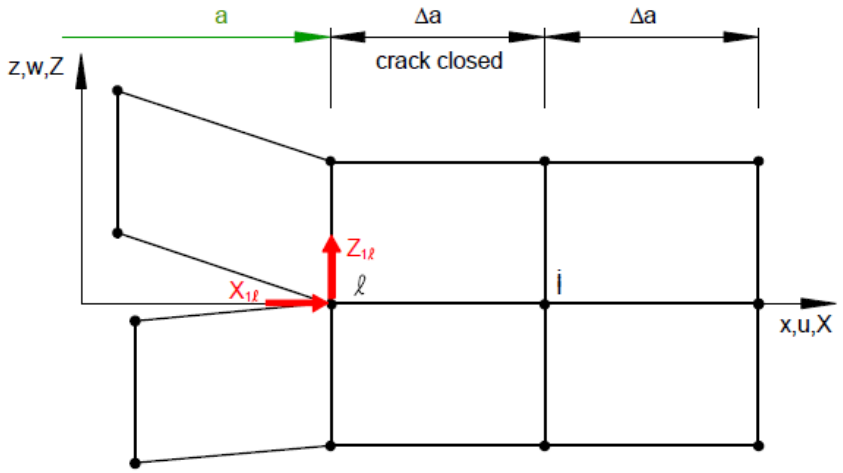

Fig. 2 First step- crack closed [15]

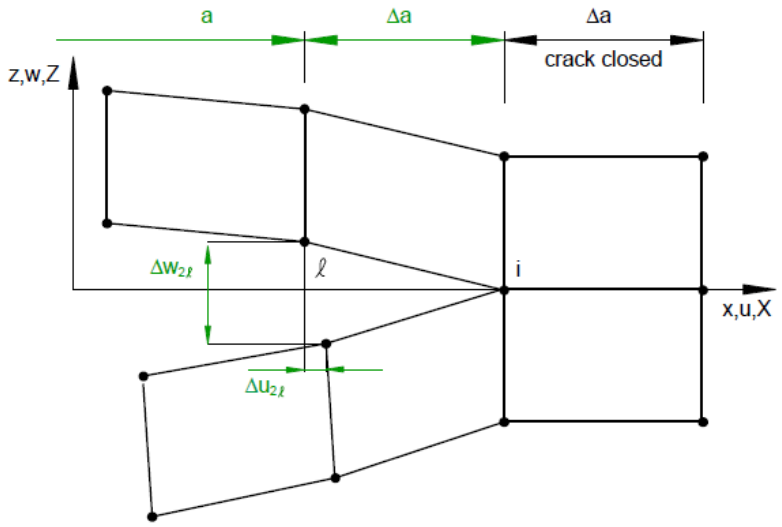

Fig. 3 Second step- crack extended [15]

where X_{1l} and Z_{1l} are the shear and opening forces at nodal point $\boldsymbol{\ell}$ to be closed, as seen in figure 2, and Δu_{2l} and Δw_{2l} are the differences in shear and opening displacements at node $\boldsymbol{\ell}$. The forces X_{1l} and Z_{1l} can be obtained from a first finite element analysis where the crack is closed and the displacements Δu_{2l} and Δw_{2l} are obtained from a second finite element analysis, where the crack has been extended to its full length.

The VCCT is based on the same assumptions as the two-step VCCT, but the difference is that the displacements behind the crack tip at node i, are approximately equal to the displacements behind the original crack tip at node $\boldsymbol{\ell}$.

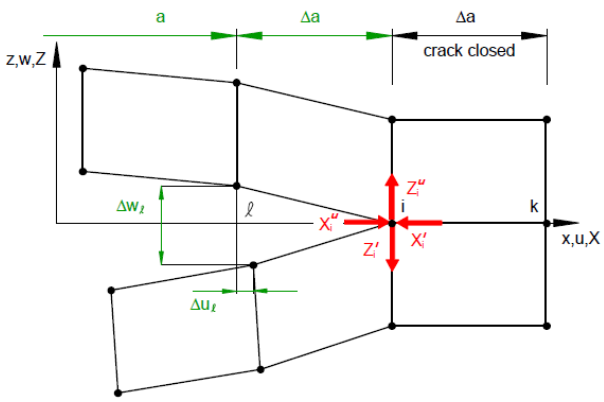

Fig. 4 One step-VCCT [15]

The energy released when the crack tip is extended by Δa from $a + \Delta a$ to $a + 2\Delta a$ is identical to the energy required to close the crack between location i and k. The formula for VCCT is the following:

$$G_{equiv} = \frac{1}{2}[X_i * \Delta u_l + Z_i * \Delta w_l] \tag{9}$$

where X_i and Z_i are the shear and opening forces at nodal point i and Δu_i and Δw_i are the shear and opening displacements at node $\boldsymbol{\ell}$ as seen in figure 4. The forces and displacements required to calculate the energy G_{equiv} to close the crack may be obtained from one single element analysis.

The fracture criterion used for all the experiments that involved VCCT was the power law criterion. The power law model is described by Wu [20] with the following formula:

$$\frac{G_{equiv}}{G_{\ equivc}} = \left(\frac{G_I}{G_{IC}}\right)^{a_m} + \left(\frac{G_{II}}{G_{IIC}}\right)^{a_n} + \left(\frac{G_{III}}{G_{IIIC}}\right)^{a_o} \tag{10}$$

where $Gequiv$ is the equivalent energy release rate, and $Gequivc$ is the critical energy release rate. For using this fracture criteria, one must provide the critical energy release rate for the different types of loadings and provide a_m ,a_n, and a_o, which are exponents used to decide if a linear or non-

linear model will be used. This is an empirical relation based on experimental observations by Wu, he did the following statement: “The crack propagates along an essentially straight line but makes microscopic skips across neighboring glass fibers." In his paper he proposed two approaches, but this relationship fitted the data from the experiments he realized.

2.2.2 CZM

Although it is not part of this study, an introduction to CZM is offered because later, cohesive segments will be introduced with X-FEM. CZM has gained considerable attention over the past decade, as it represents a powerful yet efficient technique for computational fracture studies. The early conceptual works related to CZM date back to the early 60's and were carried out by Barenblatt, who proposed the CZM to study perfectly brittle materials and Dugdale, who adopted a fracture process zone concept to investigate ductile materials exhibiting plasticity [18]. Cohesive zone elements do not represent any physical material, but describe the cohesive forces which occur when material elements are being pulled apart [11]. One of the advantages that cohesive elements present is that an initial flaw is not needed, so cohesive elements are implanted at potential failure sites and are introduced a softening traction/separation behavior, as seen in figure 5, allowing the onset of a crack when the criteria is met . Fracture mechanics is indirectly introduced because the area under the softening curve is equated to the critical fracture energy [12].

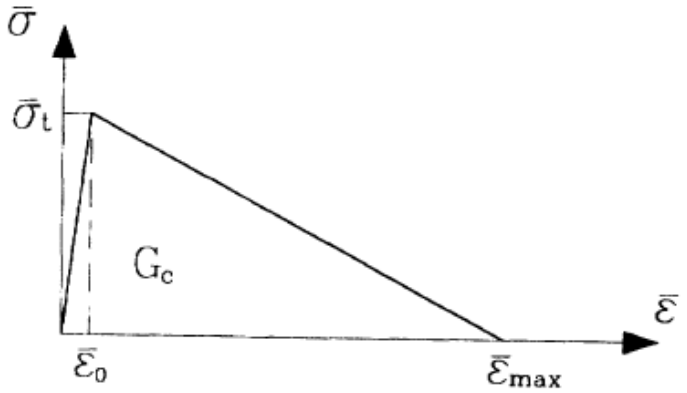

Fig. 5 Traction/displacement relationship [12]

Further reading is encouraged to get a better understanding of CZM, there are a lot of aspects in this area that need special attention to do a proper cohesive zone modeling.

2.3 X-FEM

The extended finite element method (X-FEM) is a numerical technique that extends the classical finite element method by enriching the solution space for solutions to differential equations with discontinuous functions [2]. The extended finite element method was first introduced by Belytschko and Black [8]. With X-FEM you can study the onset and crack propagation in quasi-static problems, one of the advantages of the method, is that it allows you study crack growth along an arbitrary, solution-dependent path without the needing to remesh the model [9].

For fracture analysis, the enrichment functions typically consist of the near-tip asymptotic functions that capture the singularity around the crack tip and a discontinuous function that represents the jump in displacement across the crack surfaces [2]. Approximation for a displacement vector function u with the partition of unity enrichment is

$$u = \sum_{I=1}^{N} N_I(x)[u_I + H(x)a_I + \sum_{\alpha=1}^{4} F_\alpha(x) b_I^\alpha] \tag{11}$$

Where $N_I(x)$ are the usual node shape functions; the first term on the right-hand side of the above equation, u_I is the usual node displacement vector associated with the continuous part of the finite element solution; the second term is the product of the nodal enriched degree of vector,a_I, and the associated discontinuous jump function $H(x)$ across the crack surfaces; and the third term is the product of the nodal enriched degree of freedom vector, b_I^α, and the associated elastic asymptotic crack-tip functions, $F_\alpha(x)$. Figure 6 gives a more clear understanding of formula number 11.

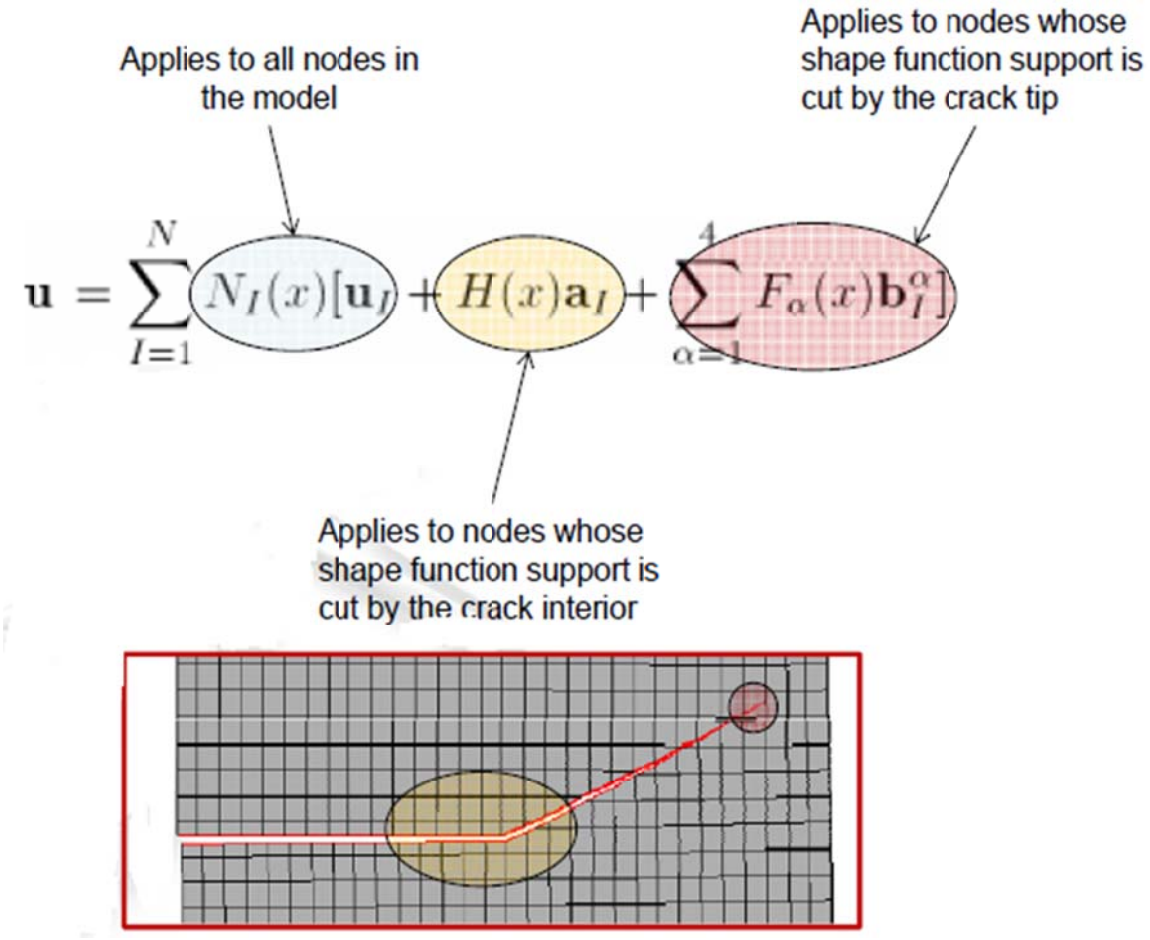

Fig. 6 X-FEM concepts [2]

So in other words, the crack can grow through the elements, elements that are partitioned create sub-elements by additional nodes. ABAQUS call these nodes phantom nodes, which are nodes superposed to the original ones. When the element is cut through the crack, real and phantom nodes are no longer tied together and can move apart.

2.4 J-INTEGRAL

The J-integral was first introduced by Rice [17]. For a 2D configuration, the J integral can be written as:

$$J = \int_{\Gamma} \left(W dy - T \frac{\partial u}{\partial x} ds\right) \tag{12}$$

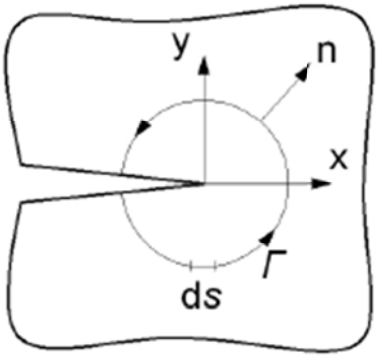

Fig. 7 Arbitrary contour path enclosing the crack tip

Here Γ is a curve surrounding the notch tip, the integral being evaluated in a counterclockwise sense starting from the lower flat notch surface and continuing along the path Γ to the upper flat surface. T is the traction vector defined according to the outward normal along Γ, Ti=σijnj, u is the displacement vector, and ds is an element of arc length along Γ.

The J-integral can be viewed as a parameter which characterizes the state of affairs in the region around the crack tip [8]. The fundamental properties of J are the following:

- *J* is a path independent for linear or nonlinear elastic material response
- *J* is equal to $= -\frac{d\Pi}{dA}$ for linear or nonlinear elastic material response
- *J* is equal to G
- *J* can easily be determined experimentally
- *J* can be related to the crack tip opening displacement δ

Because of the mentioned properties, J has been proposed as an attractive candidate for fracture criterion. The properties were derived under elastic material response. Attempts have been made to extent the realm of applicability of the J-integral fracture criterion to ductile fracture where extensive plastic deformation and possible stable crack growth precede fracture instability.

3. METHODOLOGY

3.1 MODE I PROPAGATION

For modeling crack growth in mode I, a DCB specimen was chosen. The DCB is an attractive configuration for the study of crack propagation and arrest, both from the experimental and theoretical points of view [10], figure 8 shows the configuration of the specimen.

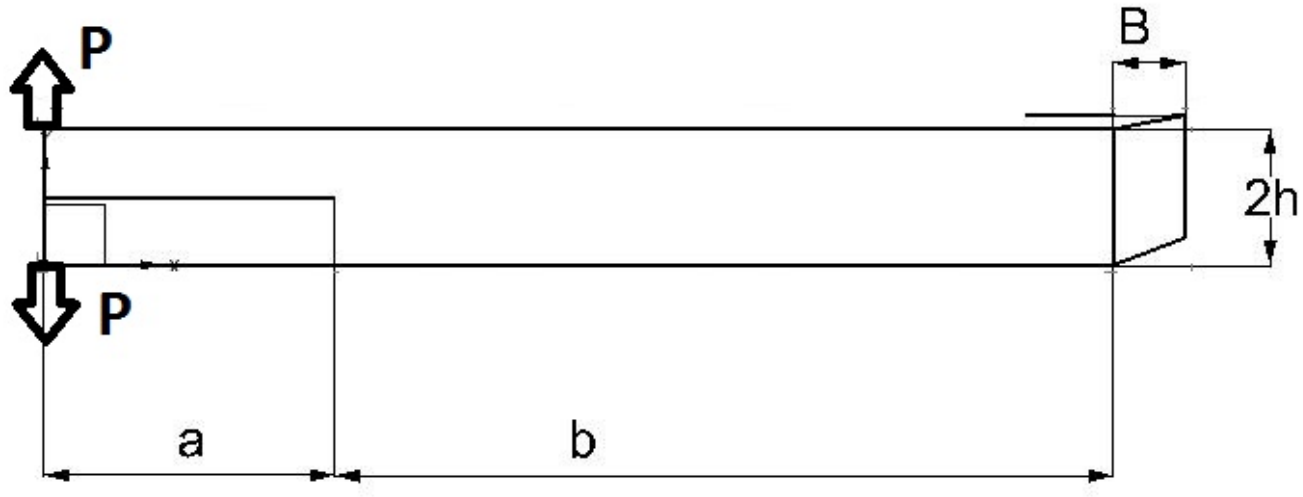

Fig. 8 Double cantilever beam specimen

The dimensions used in this study were the following:

a= 0.2 meters

b= 0.6 meters

2h= 0 .03 meters

B= 0.2 meters

The dimensions for this specimen were chosen randomly, only taking into account that the dimensions for initial flaw, thickness, and length were valid within the range of linear elastic fracture mechanics and a plane strain condition was present.

The dimensions requirement for this validation was obtained using the following equations:

$$a \geq 2.5 \left(\frac{K_{IC}}{\sigma_Y}\right)^2 \tag{13}$$

$$B \geq 2.5\left(\frac{K_{IC}}{\sigma_Y}\right)^2 \tag{14}$$

$$W \geq 2.5\left(\frac{K_{IC}}{\sigma_Y}\right)^2 \tag{15}$$

These equations according to the American Society for Testing Materials (ASTM) [6], ensures that the thickness requirement gives nearly plane strain conditions at the tip, while the on in-plane dimensions ensure that the normal behavior is elastic and that K_I characterizes crack tip conditions.

The material properties used for the model were chosen to mimic AISI 4340 steel; the stress intensity factor K_I is the only property that was modified to have a tougher material. There was no special criterion for this property change other than see how a tougher metal behaved in the numerical model. Table 1 shows the principal material properties used.

Table 1. Material properties of mode I specimen

Properties	**Value**	**Units**
Critical energy release rate	20000	$\frac{J}{m^2}$
Critical stress intensity factor	65000000	$Pa * \sqrt{m}$
Elastic modulus of elasticity	200000000000	Pa
Yield strength	472000000	Pa

Now that the dimensions and the properties of the model had been introduced, the beam theory used to benchmark ABAQUS is explained.

There is more than one analytical model for a DCB, one example is based on a linear elastic foundation proposed by Kanninen [10], but for this study a simple beam theory without any type of sophistication was used. In the recommendations section, other analytical solutions are discussed.

For the simple beam theory model, the two arms are considered as cantilevers with zero rotation at its ends. With this assumption in mind, the equations used for the model were the following:

$$Gc = \frac{3u^2Eh^3}{16\eta a^4} \tag{16}$$

where $\eta = 1 - \upsilon^2$ is used for plane strain; υ is the Poisson's ratio

From this equation, variable a was the desired crack extension length and we solved for u in order to find the displacement needed to increase the crack. For this study, the goal was to propagate the crack 0.3 meters from the initial flaw making the complete crack length equal to 0.5 meters.

Once the displacement u was found, it was important to consider that this displacement is not for a single arm so:

$$u' = \frac{u}{2} \tag{17}$$

when u' was found, simple beam theory was applied to get the force for the onset of crack growth. This was done by using equation 18, where a needed to be the size of the initial flaw.

$$P = \frac{1}{\eta}\frac{u'3EI}{a^3} \tag{18}$$

where I is equal to:

$$I = \frac{Bh^3}{12} \tag{19}$$

Based on the dimensions and properties of the model, the necessary applied displacement to growth the crack the desired amount was $u' = 0.049$ meters.

Once the problem was defined, a 2D model was set-up in ABAQUS/STANDARD. An implicit scheme was used with a mesh size of 0.001 meters, quadrilateral first order elements were used with the formulation CPE4I. Figure 9 shows the mesh used for the simulation; 24,000 elements were created with the mentioned mesh size, simulations with finer meshes were done, but the results were comparably equal and the time consumed for a finer mesh analysis was greater with no extra benefit at all.

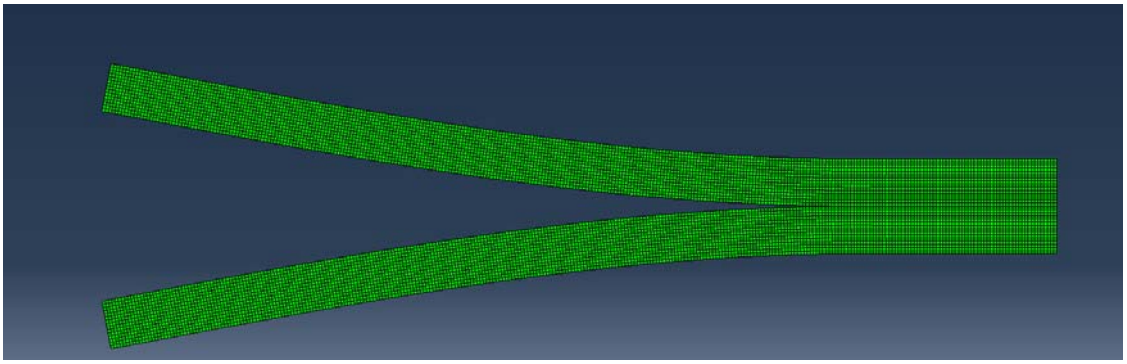

Fig. 9 Mesh used for mode I propagation

The initial step size was set to be .001, the minimum to be 1E-020, and a maximum of .001 was used during the applied displacement step. For a VCCT analysis, small time increments are required. ABAQUS track the location of the active crack front node by node; therefore the crack is allowed to advance a single node at the time in any single increment. This is the reason why the initial and maximum time step are so small; the same parameters for time step was used with the other two techniques: X-FEM coupled with VCCT and X-FEM with cohesive segments.

The boundary conditions applied for this model are shown in figure 10; these boundaries are: the applied displacement and a restriction in movement in the x-axis where the applied displacement is located in order to prevent rotation. This configuration resembles the arrangement of the classical fixed cantilever beam, where a displacement is applied at the free end and in the opposite side there is a wall.

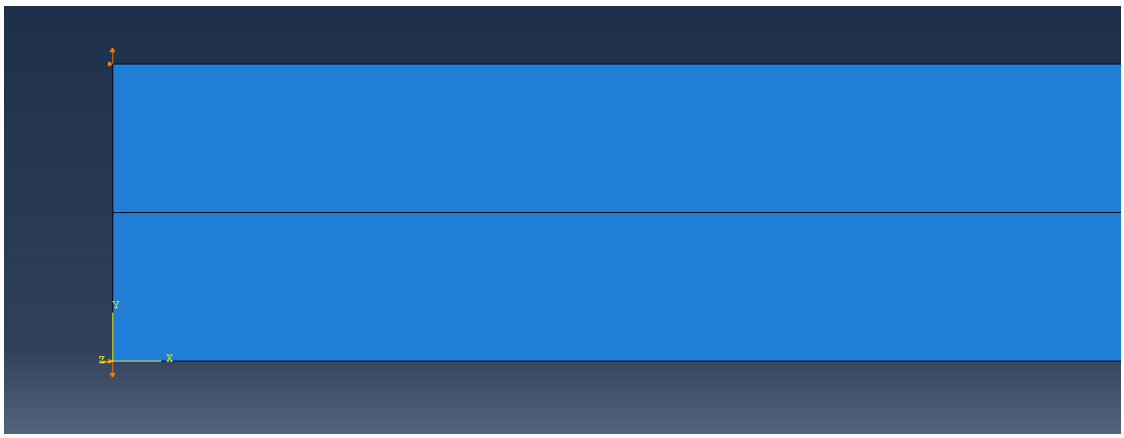

Fig. 10 Applied boundary conditions

Now that the basic parameters for the model have been introduced, the set-up of the fracture mechanics routines is presented.

3.1.1 VCCT

The VCCT as mentioned in chapter 2, is a technique that helps us simulate crack propagation. As mentioned in [2], crack propagation problems using VCCT criterion are numerically challenging. In order to help overcome convergence issues during the propagation, ABAQUS provides three different types of damping to aid convergence for the model: contact stabilization, automatic stabilization and viscous regularization. For this study, only viscous regularization was used based on the comments of Ronald Krueger [14]. Viscous regularization in ABAQUS is based on a Duvaut-Lions regularization scheme.

Viscous regularization is applied only to nodes on contact pairs that have just debonded. The viscous regularization damping causes the tangent stiffness matrix of the softening material to be positive for sufficiently small time increments, other reason why small time steps were used [2]. The recommendation for use viscous regularization in models when convergence become difficult is to set the damping parameters to relatively high values and rerun the analysis, for this study the parameters were chosen based on a iterative procedure to see which values would help to converge the model. When using viscous regularization, is necessary to monitor the energy absorbed by viscous damping, this is done by checking the viscous damping *ALLVD* against the total stain energy in the model *ALLSE*, the criterion used for this study was to ensure that no more that 3% of *ALLVD* vs. *ALLSE* was used. Table 2 shows the values used and the results that were obtained.

Table 2. Damping parameters for mode I VCCT

VISCOUS REGULARIZATION	CONVERGE	STEP OF FAILIURE
None	No	0.59
1E-06	Yes	NA
1E-08	Yes	NA

To model the initial flaw *a*, a seam line was used. The definition of seam crack according to ABAQUS manual 6.11 is the following; "A seam defines an edge or a face with overlapping nodes that can separate during an analysis." Figure 11 show a representation of a seam line:

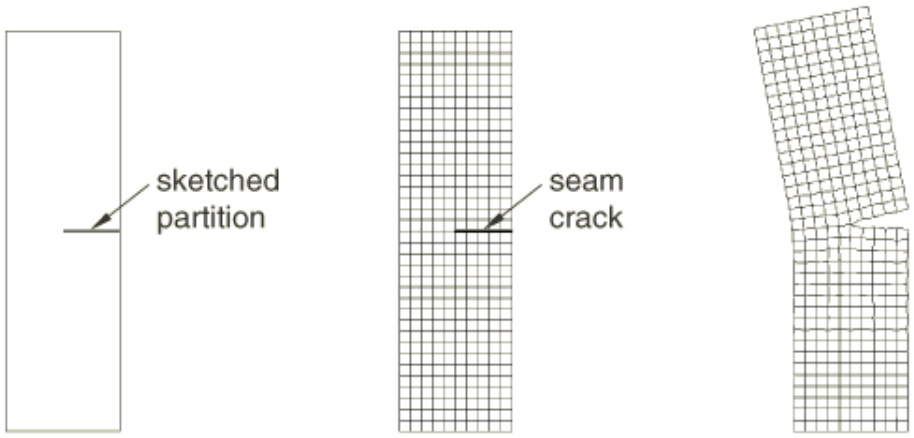

Fig. 11 Seam Crack [2]

A master surface, slave surface, and a contact formulation need to be defined to perform a VCCT analysis; for this study, a finite sliding, node to surface (default contact formulation) was used. The mentioned aspects are the more relevant to the use of VCCT. Load/displacement plots are presented in the next chapter.

3.1.2 X-FEM VCCT

For X-FEM coupled with VCCT, the set-up of the fracture mechanics routine was similar to VCCT, one of the biggest advantages found was that the routine for X-FEM VCCT was more straightforward to implement than VCCT. The difference between VCCT and X-FEM VCCT is that the latter one can be used to simulate crack propagation along an arbitrary, solution-dependent path without the requirement of a pre-existing crack in the model. The process used for model mode I propagation consisted in specify three parameters: a crack domain, define crack growth, and the direction criterion for growth. Figure 12 shows how ABAQUS presents the crack domain.

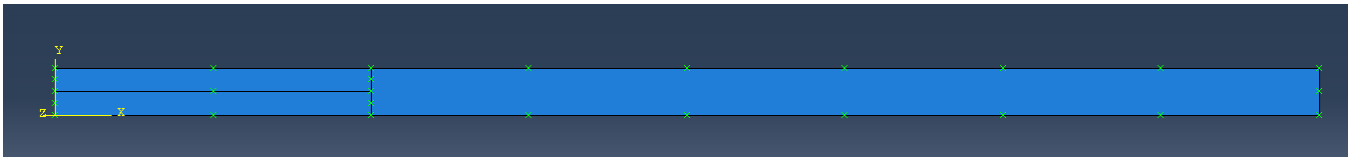

Fig. 12 X-FEM crack domain

Viscous regularization was used to assist convergence as the material fails. The damping parameters used were similar as the ones for VCCT; viscous damping against total strain energy was checked in order to ensure the model was correct. Table 3 shows the results obtained.

Table 3. Damping parameters for mode I X-FEM VCCT

VISCOUS REGULARIZATION	CONVERGE	STEP OF FAILIURE
None	No	0.185
1E-06	Yes	NA
1E-07	Yes	NA
1E-08	No	0.186

For this model, the initial flaw was indicated in the model, but it wasn't modeled as in VCCT. The pre-existing crack for X-FEM must be contained within the crack domain, also is important to point out that a seam crack must not be used to specify the initial flaw, the program would give back an error before it is submitted for analysis.

3.1.3 X-FEM COHESIVE SEGMENTS

X-FEM with cohesive segments was the other approach used with X-FEM; this method is based on the traction separation cohesive behavior. One difference between X-FEM VCCT and X-FEM cohesive segment is that the latter can be used for modeling brittle or ductile fracture whereas the X-FEM VCCT is recommended for brittle fracture only. The set-up for this technique consisted in defining the enriched area, as in the previous analysis, and the following criteria for crack growth: damage

initiation and damage evolution. For damage initiation and extension, ABAQUS uses the following built in models:

- the maximum principal stress criterion
- the maximum principal strain criterion
- the maximum nominal stress criterion
- the maximum nominal strain criterion
- the quadratic traction-interaction criterion
- the quadratic separation-interaction criterion

The model used for this study was the maximum nominal stress criterion, which is represented by the following equation:

$$f = \max\left\{\frac{\langle t_n \rangle}{t_n^o}, \frac{t_s}{t_s^o}, \frac{t_t}{t_t^o}\right\} \tag{20}$$

For this study, the nominal traction stress vector, t, consists of two components, t_n is the component normal to the likely cracked surface and t_s is the shear component. t_n and t_s represent the peak values of the nominal stress. Formula 21 shows the equation used for calculating the initiation parameter for the normal traction of the crack surface.

$$\sigma_{yy} = \frac{K_I}{\sqrt{2\pi r}} \tag{21}$$

For this formula we used r as the element size ahead the crack tip, the stress intensity factor was a parameter given by the material property. The value damage initiation was $\sigma_{yy} = 797810000$ Pa. Once established the damage initiation, damage evolution was specified. Damage evolution describes the rate at which the cohesive stiffness is degraded once the initiation criterion is met. For this study an energy criterion was chosen, which is based on the dissipated energy as a result of the damage process. The critical energy release specified in the previous analysis was chosen. A linear model was the used as the one seen in figure 5.

Viscous regularization of the constitutive equations defining cohesive behavior in an enriched element was used to help converge the model. Table 4 shows the results

Table 4. Damping parameters for mode I X-FEM COHESIVE SEGMENTS

VISCOUS REGULARIZATION	CONVERGE	STEP OF FAILIURE
None	No	0.185
1E-05	Yes	NA
1E-07	Yes	NA
1-E08	No	0.185

3.2 MIXED MODE I/II PROPAGATION

The mixed mode crack growth was obtained by using a mixed-mode bending (MMB) specimen, this configuration was first suggested by Reeder and Crews [16]. The test simply combines the mode I DCB and the mode II end notch flexure specimen (ENF). The relative magnitude of the two applied loads determines the mixed mode ratio at the propagation front. Figure 13 shows the configuration of the MMB specimen.

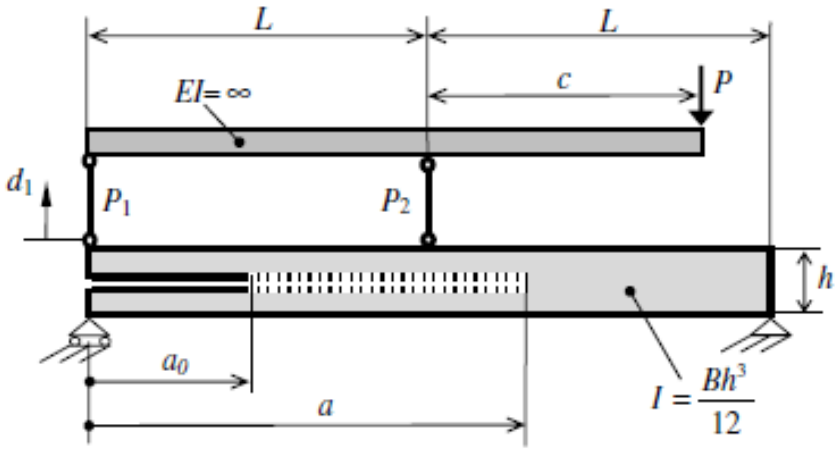

Fig. 13 MMB specimen [19]

The dimensions and properties used for the MMB specimen were exactly the same ones as for the DCB, only the addition of critical energy release rate G_{II} is added to the model which had the same value as G_I. The goal as is to propagate the crack 0.4 meters from the initial flaw. To verify that the crack had growth the desired amount, in the post-processing part of the analysis, a path was created from the first node located in the initial flaw to the last node where the crack had stopped, figure XX shows the path in the viewport. Beam theory was used to select the parameters for model the MMB in ABAQUS, the approach followed is presented in the next paragraphs.

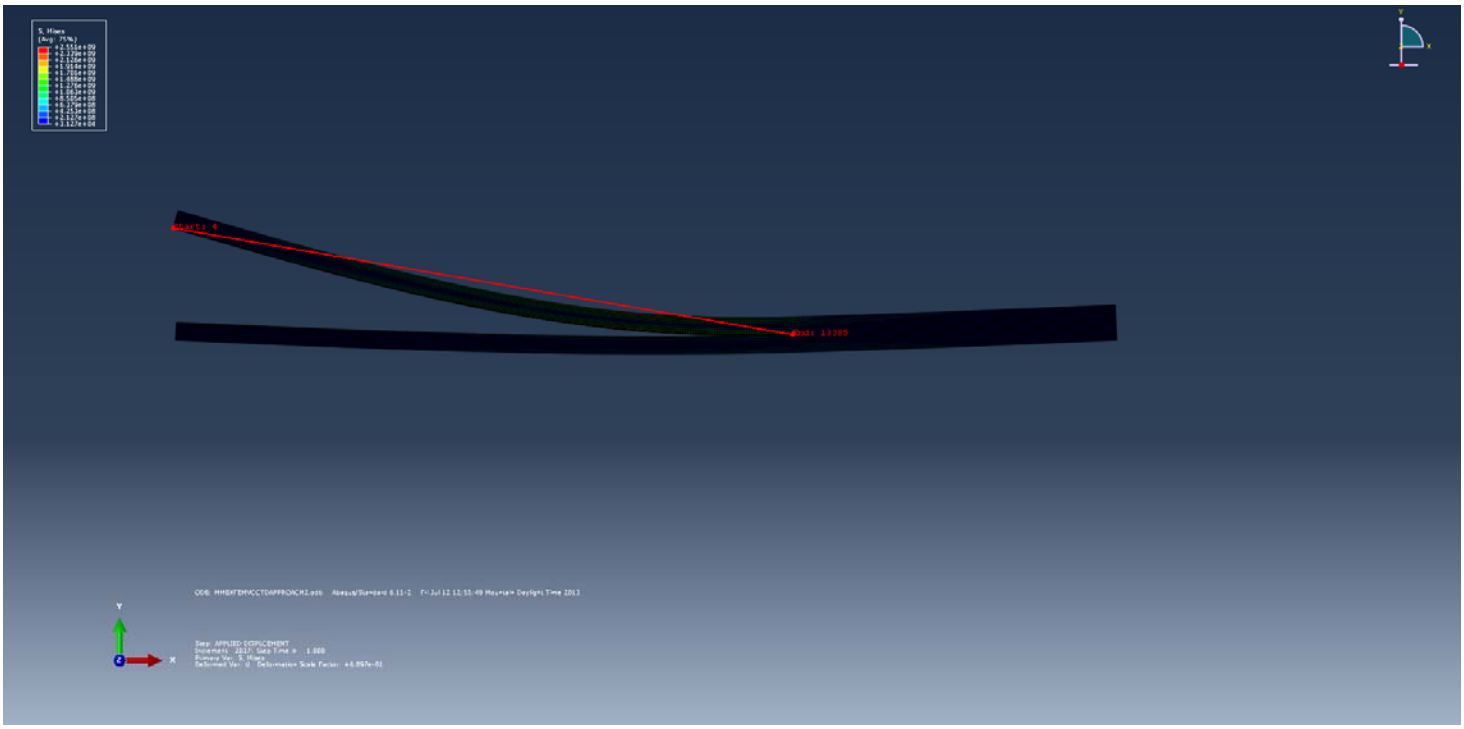

Fig. 14 Crack path

The MMB loading is represented by a superposition of simple mode I and mode II loadings equivalent to those used with DCB and ENF. Figure 15 shows how the superposition procedure incorporates beam theory equations.

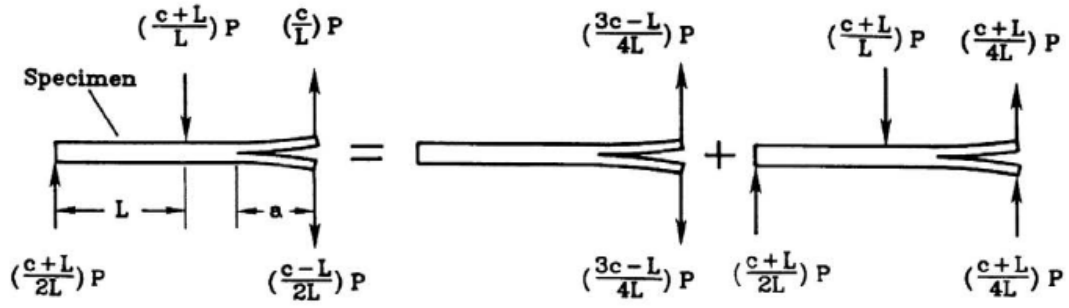

Fig. 15 Superposition for mode I and mode II [16]

For this study the desired mixed mode ratio was set to be G_{II}/G_t=0.5, where *Gt* equals $G_I + G_{II}$. The loading position c determines the relative magnitude of the two resulting loads on the specimen and therefore determines the mixed mode ratio, so the first step was to find the value of *c* for the desired ratio.

The applied load distance, *c*, was based on Tenchev and Falzon paper [19]. The reason for use their derivation is that the authors recognized that in previous publications, when the crack grows bigger than L (as seen in figure 13), the mode separation used by Reeder and Crews is not valid anymore. Based on this statement and considering that the desired crack growth goes beyond L, the proposed equations used to get the length *c* for the desired mixed mode ratio are the following:

$$G_I = \frac{P^2L^2}{BEI}\left[\frac{1}{2}\left(\frac{c}{L}-3\right)^2\left(\frac{a}{L}\right)^2+\frac{1}{2}\left(\frac{c}{L}+1\right)\left(5\frac{c}{L}-13\right)\frac{a}{L}+\left(\frac{c}{L}+1\right)\left(\frac{c}{L}+3\right)\right] \tag{22}$$

$$G_{II} = \frac{P^2L^2}{BEI}\left[\frac{3}{8}\left(\frac{c}{L}+1\right)^2\left(\frac{a}{L}\right)^2-\left(\frac{c}{L}+1\right)\left(2\frac{c}{L}+1\right)\frac{a}{L}+\frac{1}{2}\left(\frac{c}{L}+1\right)\left(5\frac{c}{L}+1\right)\right] \tag{23}$$

By knowing that the ratio must be G_I/G_{II}=1.0, we equate these two equations and set- up *a* to the desired amount of crack growth and solve for c.

Once that *c* was found, a linear mode fracture criteria was used for solve for P, this fracture criteria is essentially the power law.

$$\frac{G_I}{G_{IC}} + \frac{G_{II}}{G_{IIC}} = 1 \tag{24}$$

The value of *P* for the MMB came to be 21,184 N. Once P is known, the values for P_1 and P_2 were obtained using following equations:

$$P_I = \left(\frac{c}{L}\right) P \tag{25}$$

$$P_{II} = \left(\frac{c+L}{L}\right) P \tag{26}$$

As mentioned in the mode I analysis, control displacement is preferred in order to avoid numerical instabilities. The equations used to find out the displacement are shown next.

$$d_1 = \frac{P}{EI} \frac{\left(a^3+3a^2L-L^3\right)(L+c)-4a^3L}{6L} \tag{27}$$

where *a* is the desired crack extension. Displacement d_2 was not specified by Tenchev and Falzon, but another study performed by Kinloch, Wang, Williams and Yayla [1], explain the method to obtain the middle displacement by applying beam theory. The derived equation is the following:

$$d_2 = -\frac{PL^3}{6EI_0}\left(1 - \frac{c+L}{2L} + \frac{c}{b}\right) - AL - B_k \tag{28}$$

where

$$A = \frac{P}{6EI_O 2L}\left[\left(\frac{c+L}{L}\right)(2L-L)^3 - \left(1 - \frac{c+L}{2L} + \frac{c}{L}\right)2L^3\right] - \frac{B}{2L} \tag{29}$$

$$B_k = \frac{Pa^3}{3EI_O}\left[\frac{c}{L} - 7\left(1 - \frac{c+L}{2L}\right)\right] \tag{30}$$

$$I_O = \frac{2Bh^3}{3} \tag{31}$$

The boundary condition used for the model consisted of a fixed pin in the opposite arm of to the applied displacement, half length middle displacement in the y-axis and a roller in the opposite side from the pin. Figure 16 shows the boundary conditions

Fig. 16 Boundary conditions for MMB

Now that the model has been set- up, ABAQUS implementation is presented.

3.2.1 VCCT

Implementation of VCCT for the MMB followed the same approach as in mode I. The difference consisted that the parameter G_{II} was defined in the fracture criterion. Viscous regularization was used, table 5 shows the results

Table 5. Damping parameters for mixed mode I/II VCCT

VISCOUS REGULARIZATION	CONVERGE	STEP OF FAILIURE	Release Tolerance	NLGEOM
None	No	0.37	0.2	No
1E-02	No	0.39	0.2	No
1E-03	No	0.37	0.2	No
1E-02	No	0.44	0.5	Yes
1E-03	No	0.42	0.5	Yes
1E-04	No	0.42	0.5	Yes

From table 5 it was observed that none of the analysis converged, a lot more analysis were run but here are presented the most representatives cases. One of the causes for this behavior might be the criterion used for crack growth. In order to help converge the model, the release tolerance was modified, it helped but the model in comparison to the default tolerance, but the model still did not converge. Nonlinear geometry was activated as well in the model with greater release tolerance as indicated in

ABAQUS manual 6.11 to help converge the model but that didn't help. Same parameters were applied to X-FEM to see if there was any difficulty like the one with VCCT.

3.2.2 X-FEM VCCT

Same approach as in mode I. Viscous regularization results are shown in table 6.

Table 6. Damping parameters for mixed mode I/II X-FEM VCCT

VISCOUS REGULARIZATION	CONVERGE	STEP OF FAILIURE
None	No	0.213
1E-06	Yes	NA
1E-07	Yes	NA
1E-08	No	0.18
1E-09	No	0.15

3.2.3 X-FEM COHESIVE SEGMENTS

Same approach as in mode I. Viscous regularization results are shown in table 7.

Table 7. Damping parameters for mixed mode I/II X-FEM COHESIVE SEGMENTS

VISCOUS REGULARIZATION	CONVERGE	STEP OF FAILIURE
None	No	0.150
1E-05	Yes	NA
1E-06	Yes	NA
1E-07	No	.153

3.3 J-INTEGRAL FOR ENERGY RELASE RATE CALCULATION

The energy release rate is an important parameter in fracture mechanics since we can relate it to the stress intensity factor as seen in formula 5. In ABAQUS we can use the J-integral to calculate G based on the statement that $J = G$. The used methodology for this study is discussed next.

The specimen for this assessment was an infinite plate with an edge crack. The material properties were the same as the ones used for crack growth with the exception of the critical stress intensity factor, where $K_I = 50000\ Pa\sqrt{m}$. Figure 17 shows the edge crack specimen.

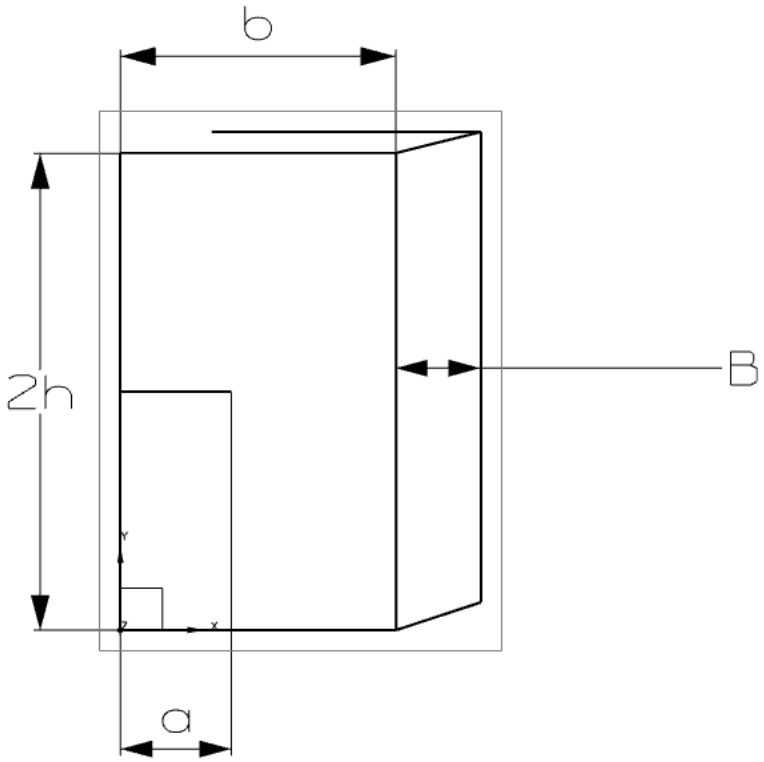

Fig. 17 Edge crack plate

where

a=0.03 meters

b=0.10 meters

B=0.05 meters

2h=0.20 meters

The boundary conditions and the loads used for this study are shown in figure 18. The boundary conditions used were two nodes fixed in the x-axis to prevent any rotation at the tips of the edge where the initial crack is located. A restriction in the y-axis in the middle of the edge opposite to the initial crack was used to ensure a mode I reading.

For determine the remote stress applied to the plate, the following formula was used were some proportions had to be met.

$$K_I = \sigma\sqrt{\pi a}\left[\frac{1+3\frac{a}{b}}{2\sqrt{\pi\frac{a}{b}}\left(1-\frac{a}{b}\right)^{\frac{3}{2}}}\right] \tag{32}$$

where

$$\frac{h}{b} \geq 1 \tag{33}$$

and

$$\frac{a}{b} \geq 0.3 \tag{34}$$

From formula 32, all the variables were known with the exception of σ. For this particular case, after solving for σ, the obtained value was $\sigma = 97475000\ Pa$.

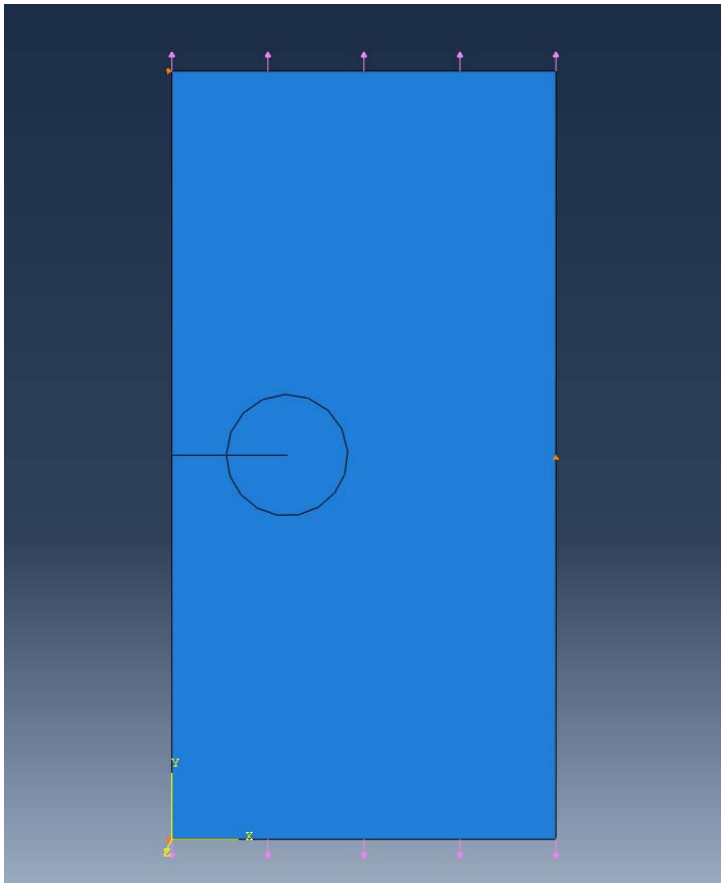

Fig. 18 Load and boundary conditions for J-integral assessment

Once the geometry, boundary conditions, and load were defined, the next step was the set-up of the contour integral analysis. The first step was to define the crack front. In a 2D analysis you can define the crack front from the three following options: a single vertex, connected edges, and connected faces; for this study the vertex option was selected.

The next step was to define crack tip; in which this case was the same vertex as in the crack front. After having defined those two parameters, the subsequent procedure consisted in specifying the crack extension. ABAQUS provides two options to specify the crack extension: normal to crack plane, n, or virtual crack extension direction, q. For this study, the virtual crack extension was defined by selecting the points from the model that represents the start and the end of the q vector, which were the beginning of the crack and the node chosen as crack front respectively. Figure 19 shows how the direction is represented in the viewport.

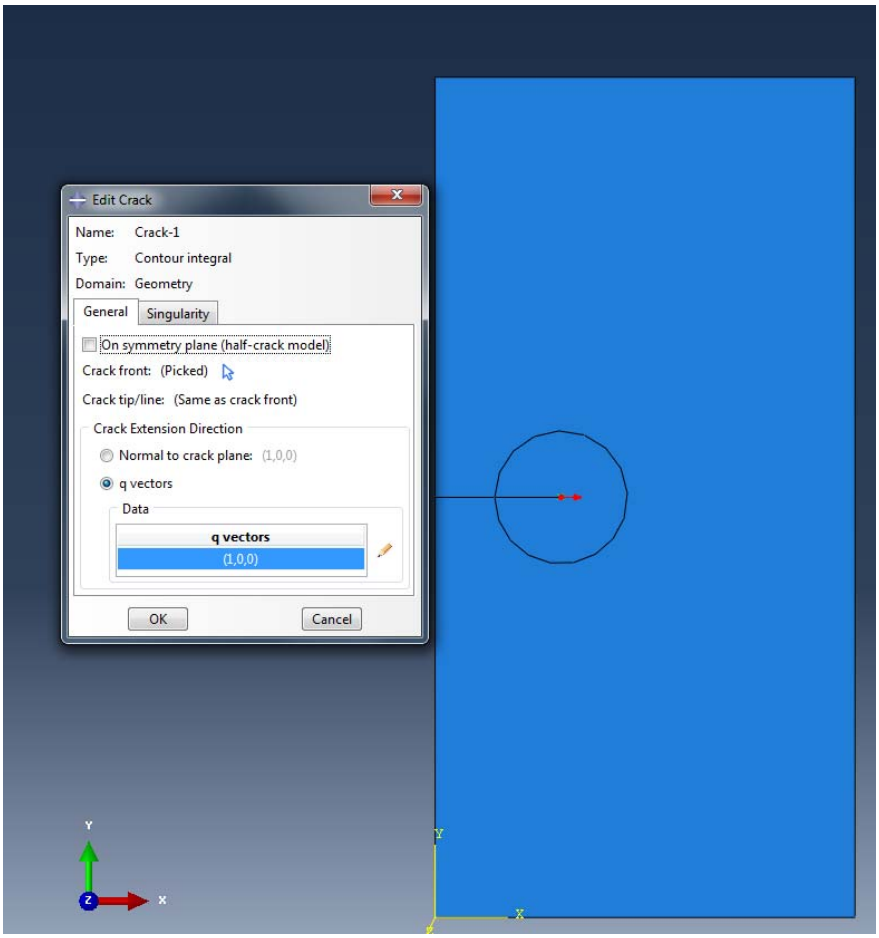

Fig. 19 q vectors

Now that the model parameters had been defined in the analysis, we have to mesh the geometry. For this analysis it was important to create the singularity in the mesh to improve the accuracy of the J-integral. Since linear elasticity is used, the singularity to capture is $\frac{1}{\sqrt{r}}$. To create the square root singularity, we need to constrain the nodes on the collapsed face of the edge to move together and move the nodes to the 1/4 points. Figure 20 shows a representation of a 2D collapsed element and figure 21 shows the actual mesh used.

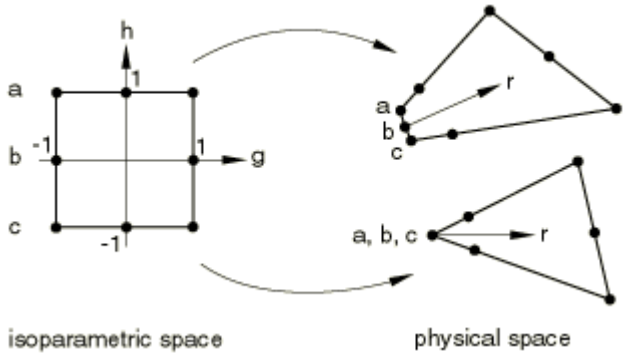

Fig. 20 Collapsed two dimensional element [2]

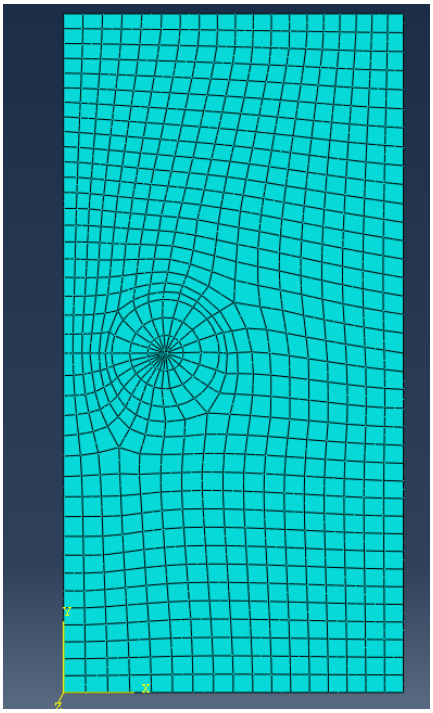

Fig. 21 Mesh used for J-integral study

An implicit scheme was selected with the default time step: 1 for initial and maximum, and a minimum of 1E-05. The element selection was CPE8 based on the plane strain assumption mentioned earlier and the quadratic formulation was used to collapse one side of the element as previously explained.

4. RESULTS

4.1 MODE I LOAD/DISPLACEMENT PLOTS

Figure 22 and 23 show the DCB in the post-processing part of the analysis in ABAQUS.

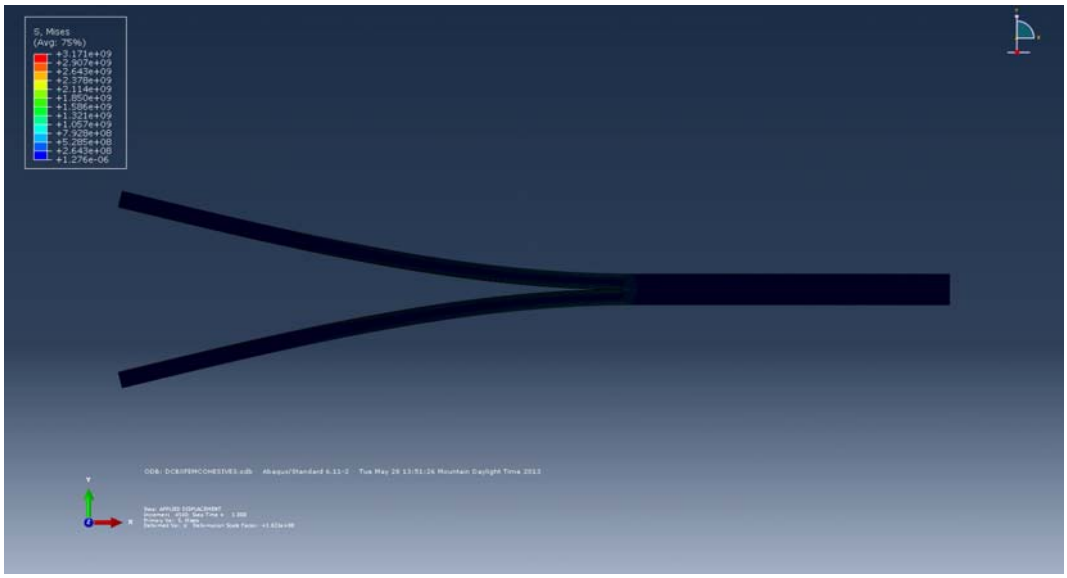

Fig. 22 DCB model in ABAQUS

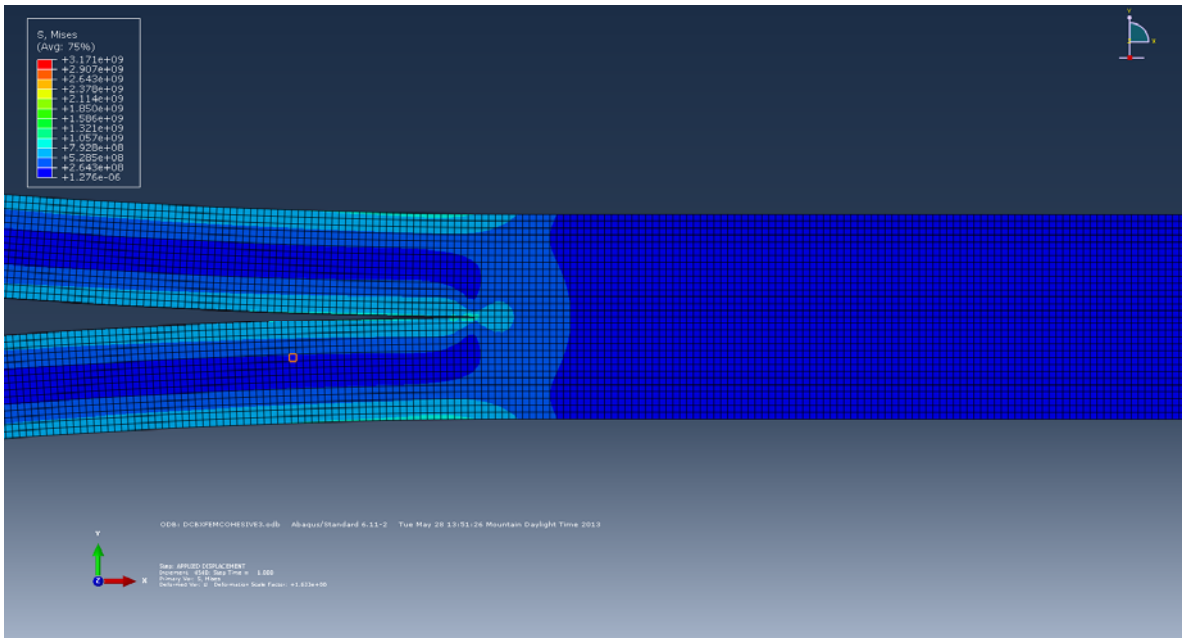

Fig. 23 Von Mises stress at the crack tip

4.1.1 VCCT PLOT

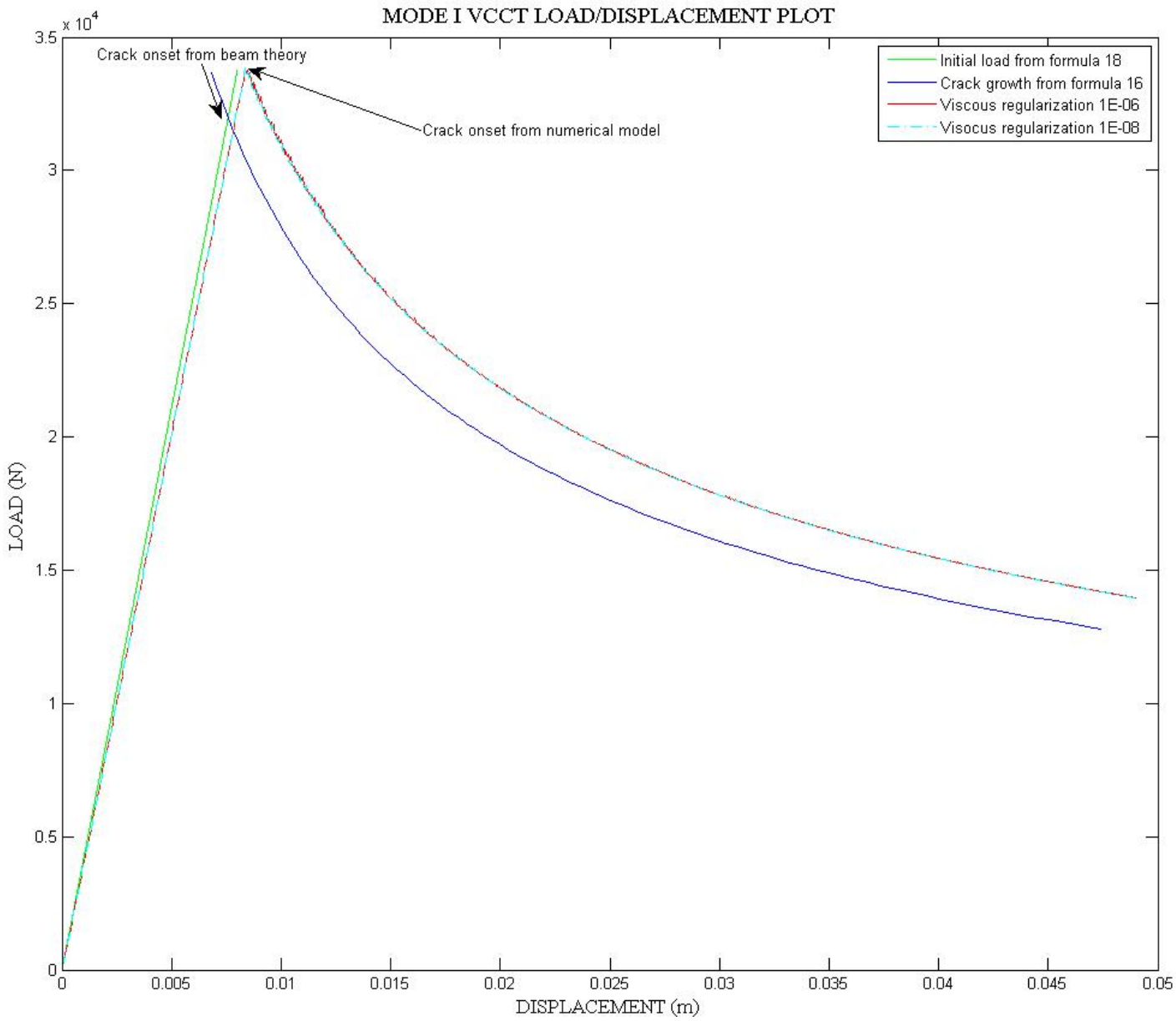

Fig. 24 Mode I VCCT load/displacement plot

Figure 24 shows the load/displacement plot for VCCT. As seen, the necessary load for initiate the crack from the analytical model is 31,997 N and from the numerically model the load obtained was 33,855 N, the difference is about 5% off from the analytical model. This solution is consistent to the solution found by Crews and Reeder [16]. This plot gives us the confidence that the implemented VCCT routine in ABAQUS is accurate since is giving us the same approximations as found by different authors in previous experiments.

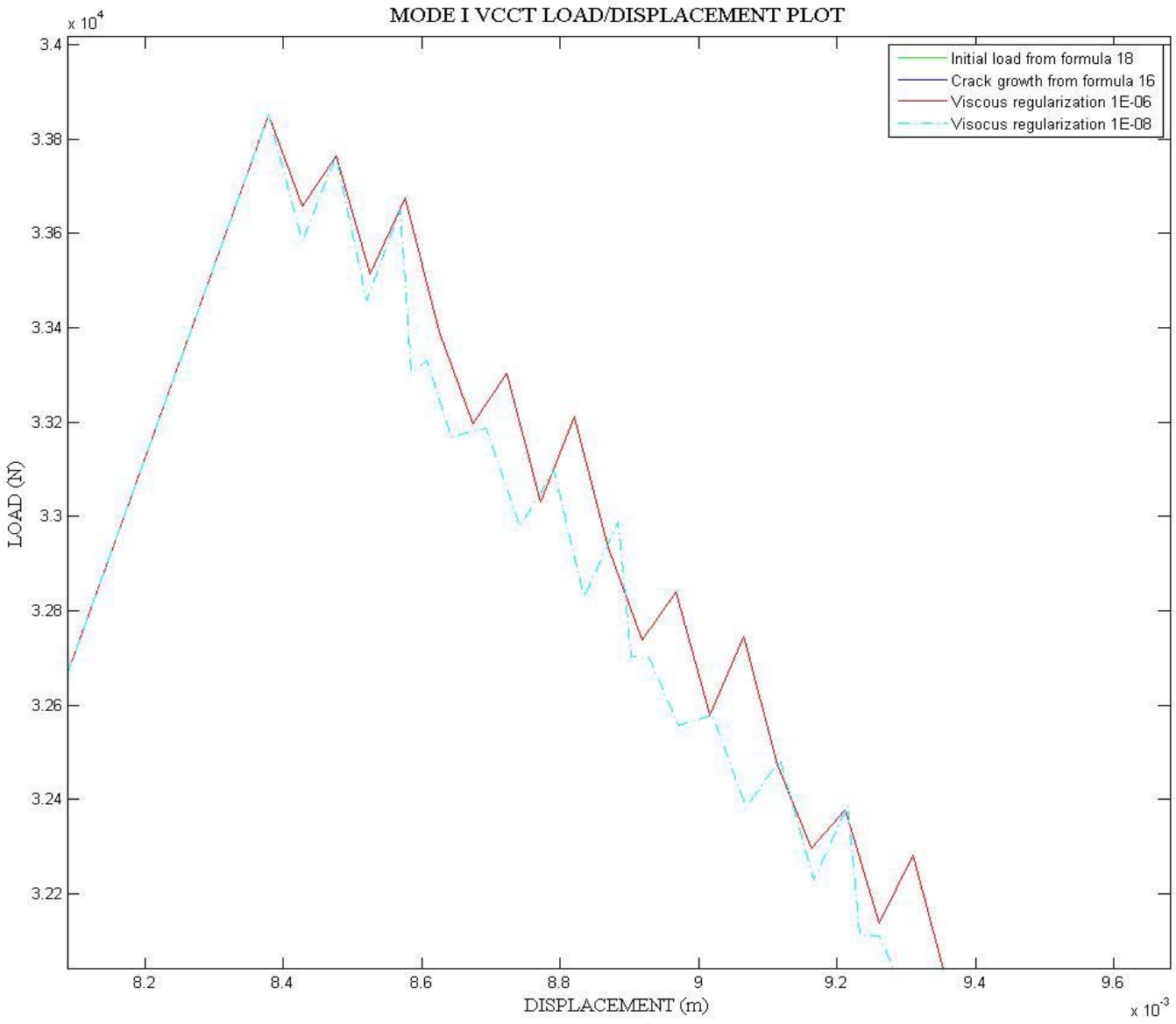

Fig. 25 Pattern difference using different viscosity for VCCT

A saw tooth pattern is seen in the plot, according to Ronald Krueger [14], this behavior appears to be dependent on the mesh size at the front of the crack. From this plot is concluded that the viscosity 1E-08 attenuate the saw tooth pattern.

4.1.2 X-FEM VCCT PLOT

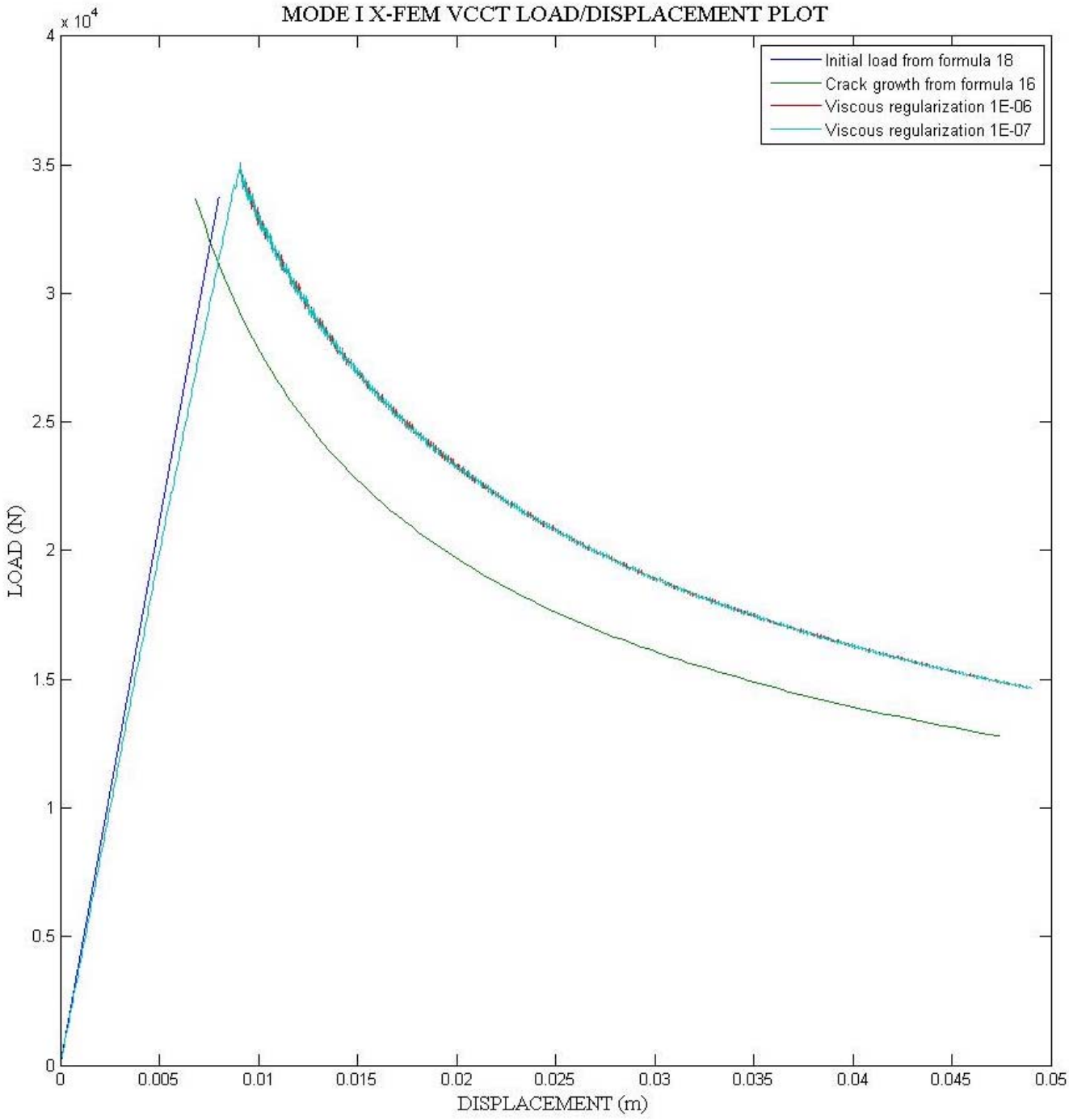

Fig. 26 Mode I X-FEM VCCT load/displacement plot

Figure 26 shows the load/displacement plot for X-FEM VCCT. As seen, the necessary load for initiate the crack from the analytical model is 31,997 N and from the numerically model the load obtained was 35,103 N, the difference is about 9% off from the analytical model. As explained earlier, this solution has the average offset seen in previous works, but an important difference is that in previous works only VCCT was used, a similar study were X-FEM VCCT was used was not found

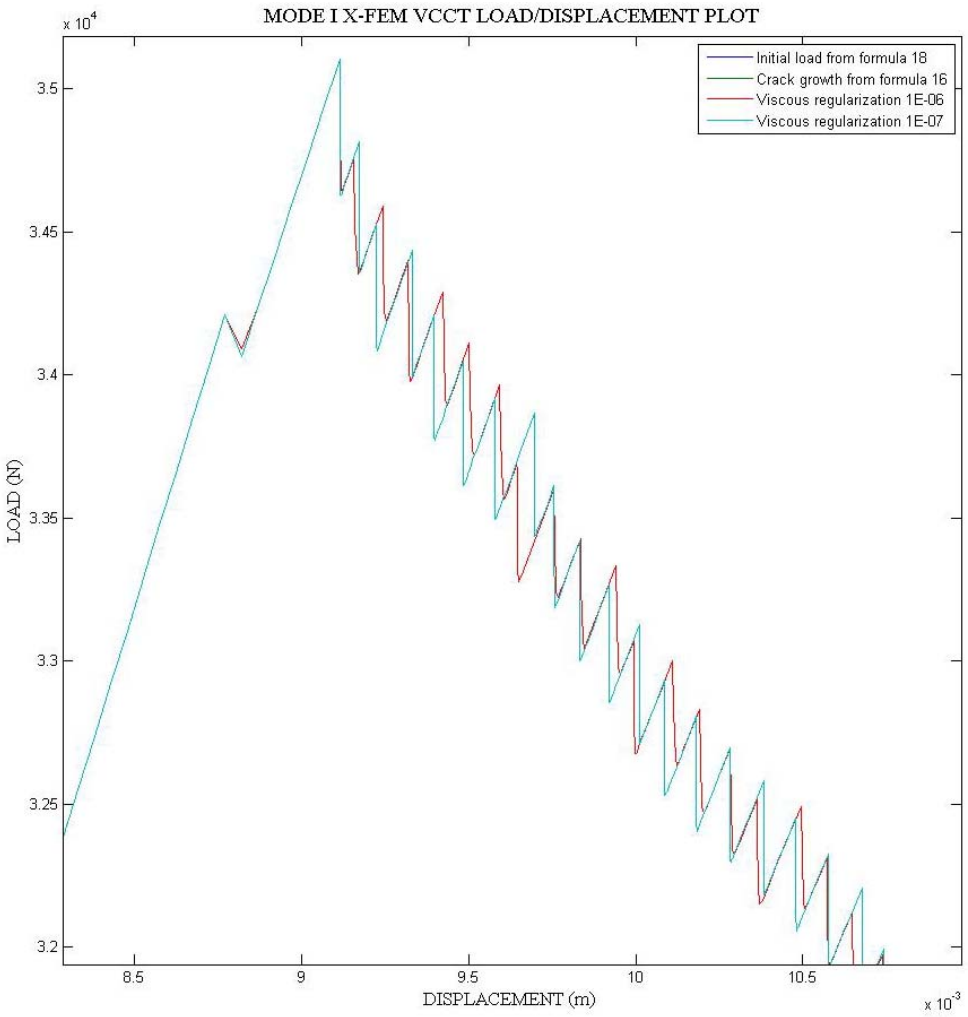

Fig. 27 Pattern difference using different viscosities for X-FEM VCCT

The saw tooth pattern is stronger with X-FEM VCCT than with VCCT.

4.1.3 X-FEM COHESIVE SEGMENTS

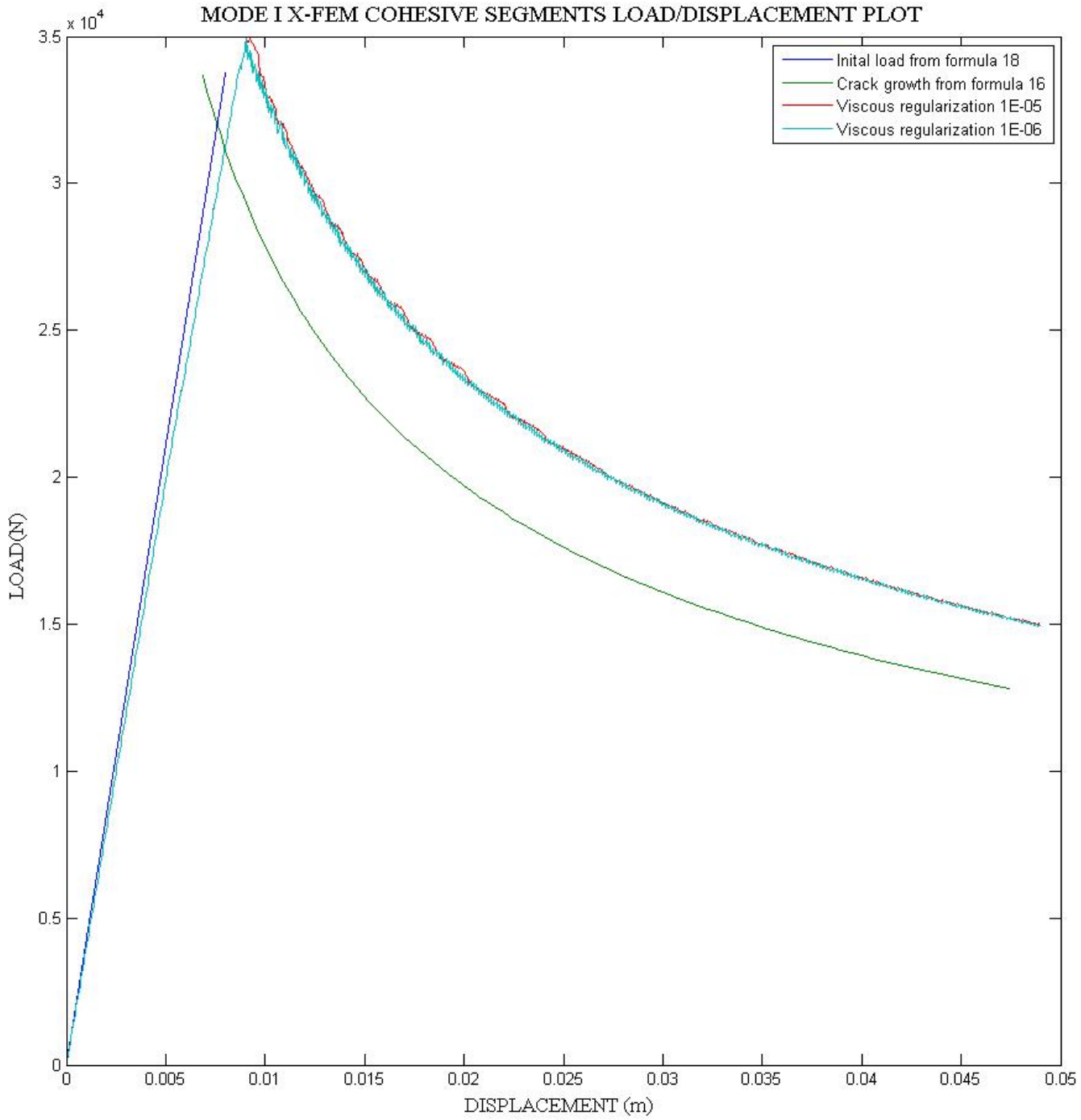

Fig. 28 Mode I X-FEM COHESIVE SEGMENTS load/displacement plot

Figure 28 shows the load/displacement plot for X-FEM VCCT. As seen, the necessary load for initiate the crack from the analytical model is 31,997 N and from the numerically model the load obtained was 34,917 N, the difference is about 9% off from the analytical model.

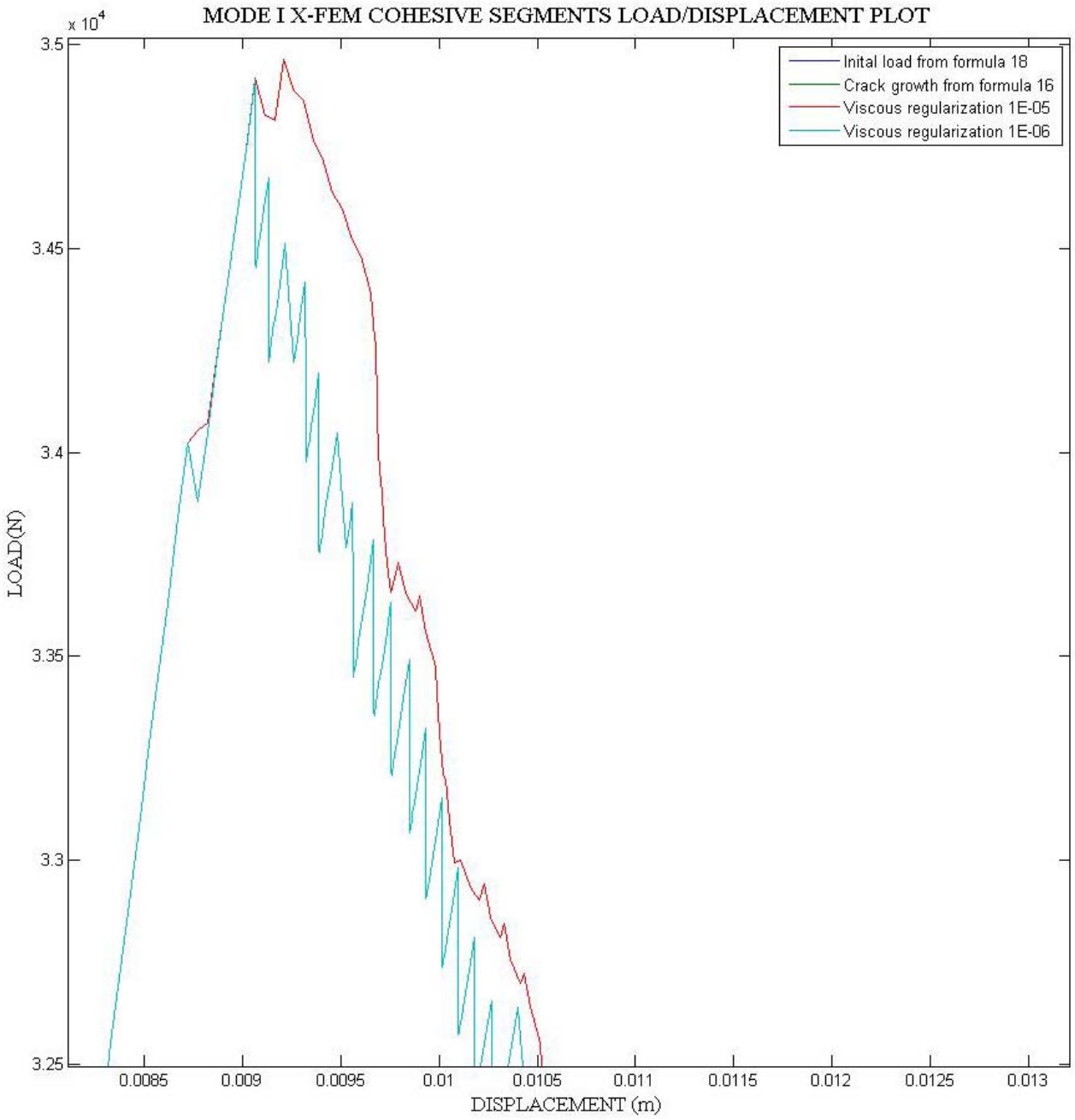

Fig. 29 Pattern difference using different viscosities for X-FEM COHESIVE SEGMENTS

Figure 29 shows the saw tooth pattern for a viscosity of 1E-06, but the following value of 1E-05 shows a totally different pattern than ones seen.

4.1.4 COMPARISON OF THE THREE TECHNIQUES

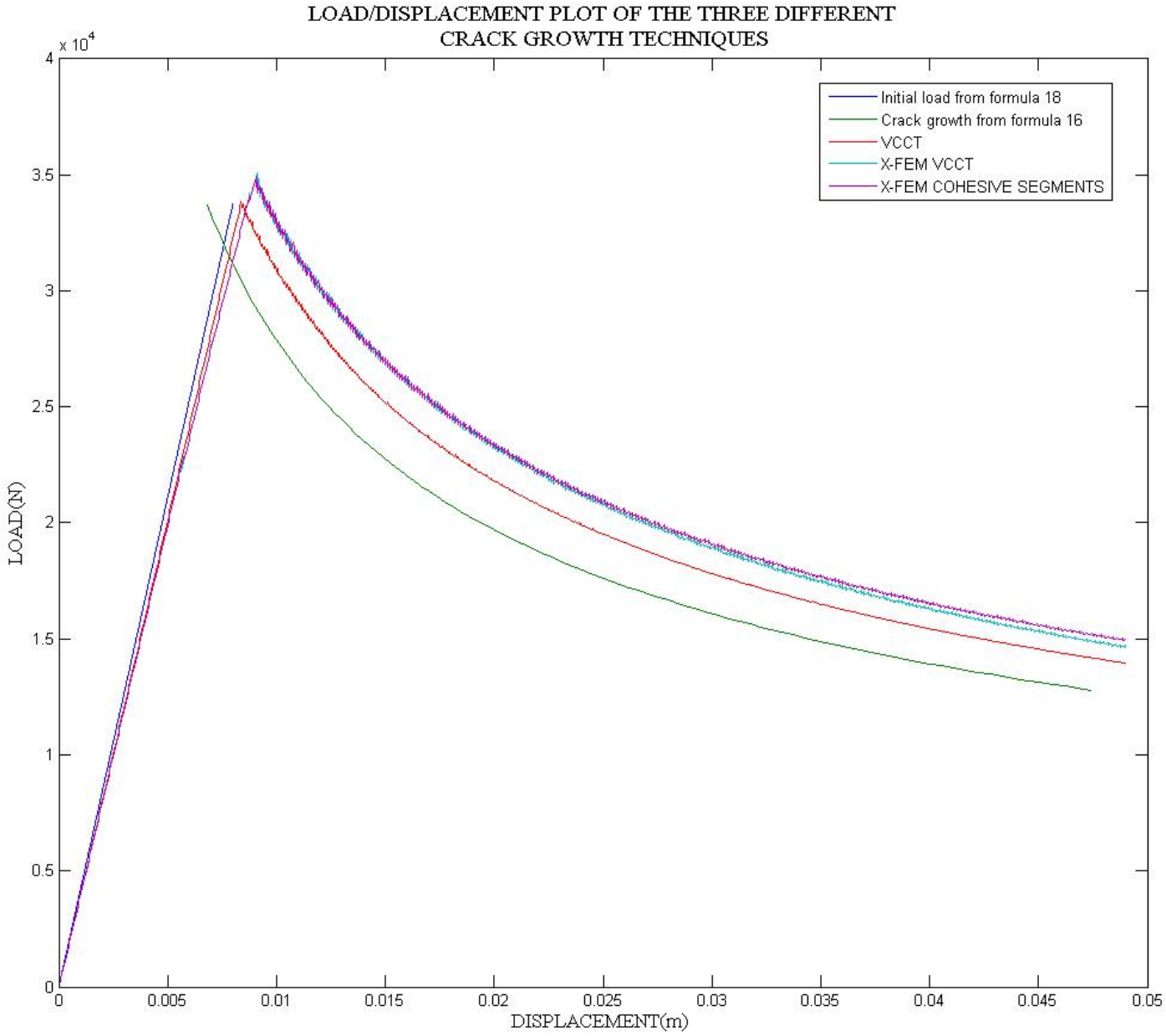

Fig. 30 Plot showing the three different techniques used.

Figure 30 shows how the initial load for delamination for both X-FEM approaches required more force than VCCT. Also is seen how X-FEM VCCT and X-FEM COHESIVE SEGMENTS have a similar pattern at the moment of crack growth. In the recommendations section, future work that can help to fit the numerical model to the closed-form analytical solution will be discussed.

4.2 MIXED MODE I/II LOAD/DISPLACEMENT PLOTS

Figure 31 and 32 show the MMB in the post-processing part of the analysis in ABAQUS

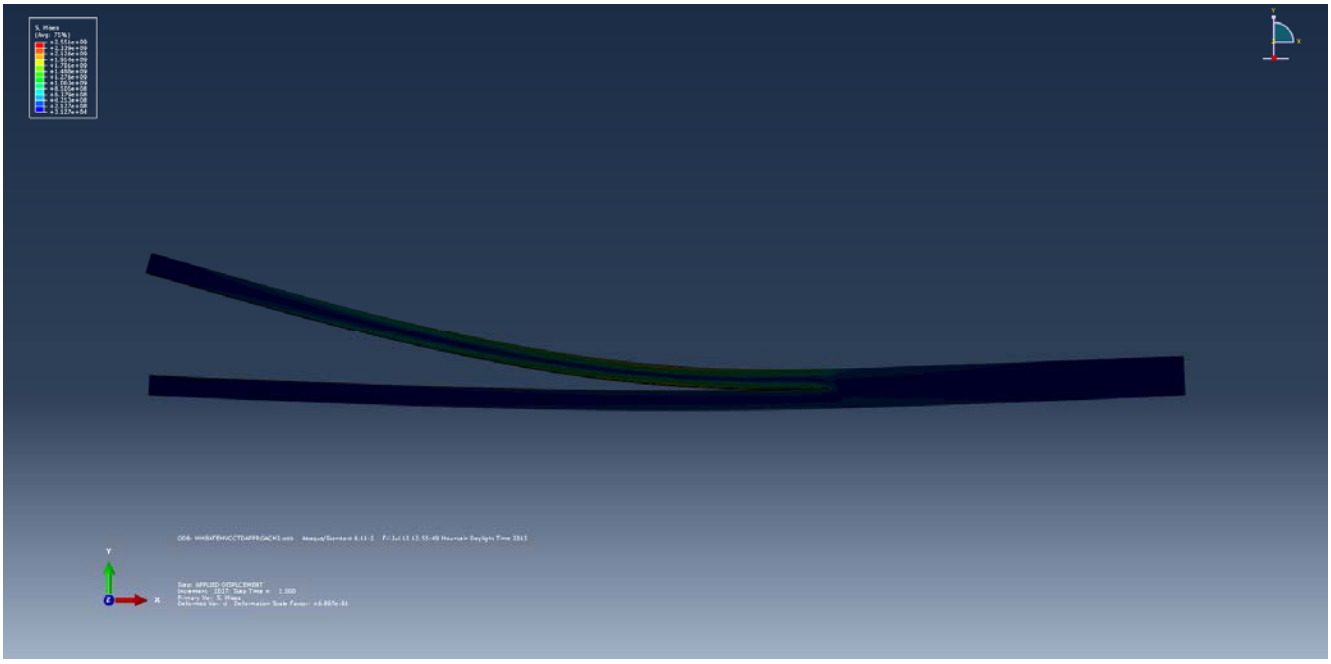

Fig. 31 MMB specimen in ABAQUS

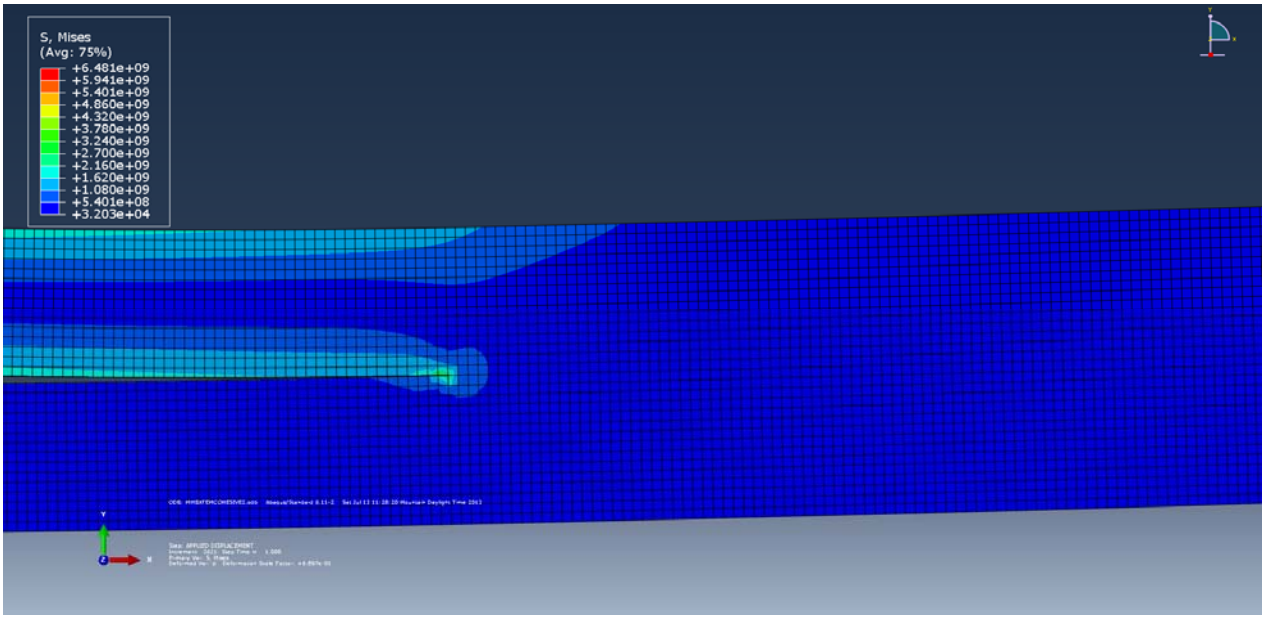

Fig. 32 Von Mises stress at the crack tip

4.2.1 X-FEM VCCT PLOT

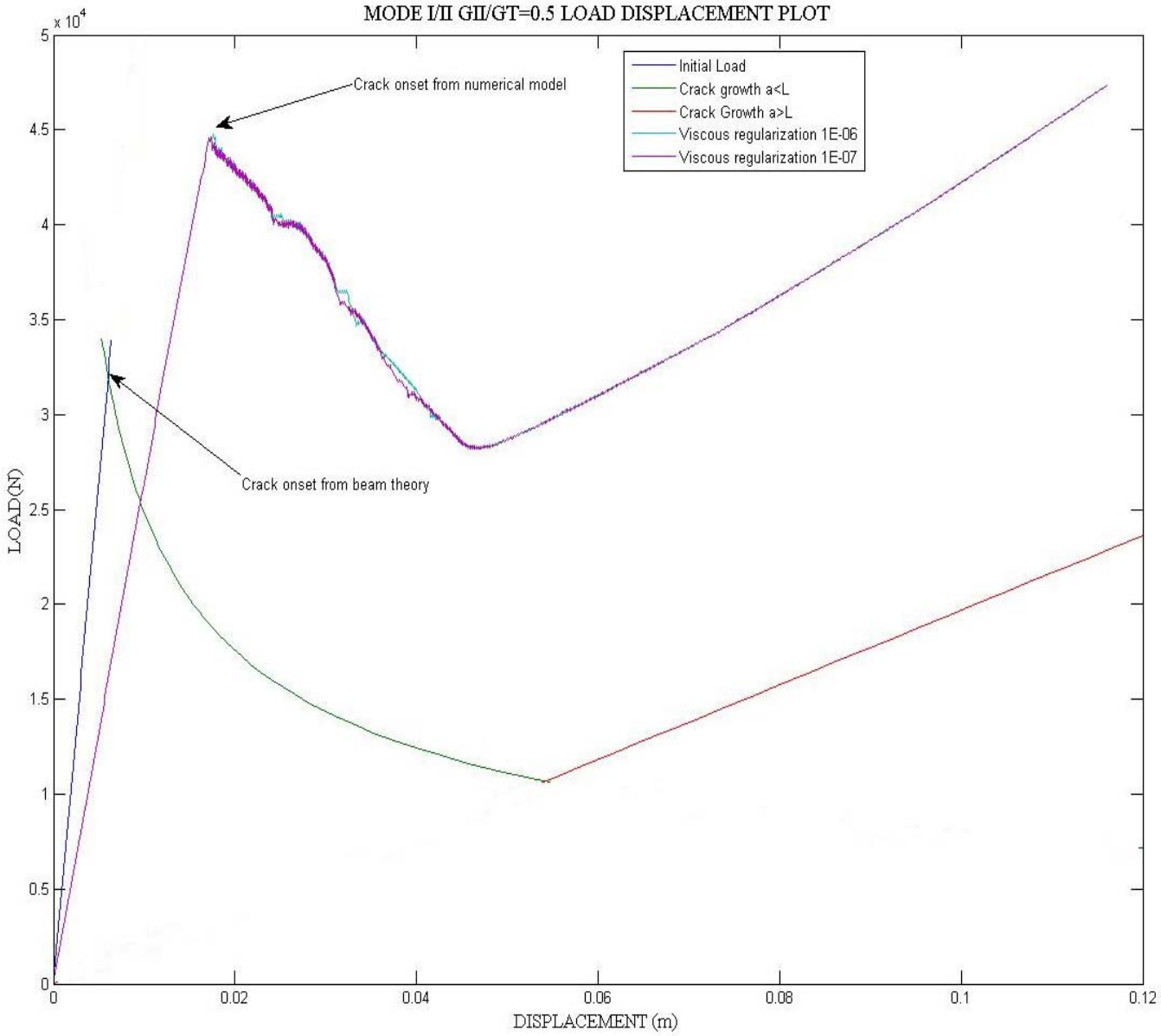

Fig. 33 Mode I/II X-FEM VCCT load/displacement plot

Figure 33 shows the load/displacement plot for X-FEMVCCT. As seen, the necessary load for initiate the crack from the analytical model is 32,019 N and from the numerically model the load obtained was 44,738 N, the difference is about 39% off from the analytical model. Further investigation is needed to decide if this percentage off comes from the numerical or analytical model.

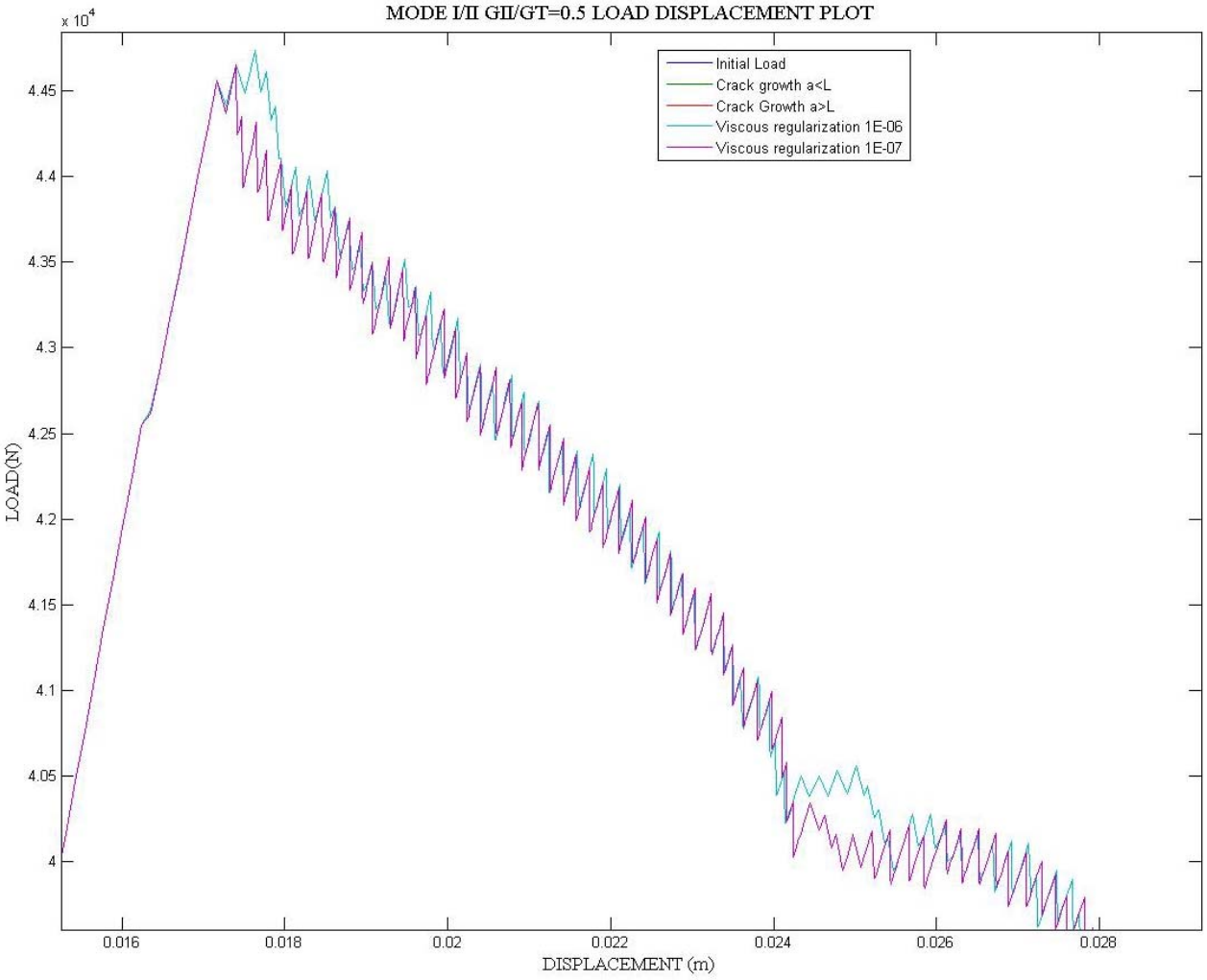

Fig. 34 Pattern difference using different viscosities for X-FEM VCCT

Same saw tooth pattern is seen in mixed mode as seen in mode I propagation, figure 34 focuses in the pattern created by using two different viscous values.

4.2.2 X-FEM COHESIVE SEGMENTS PLOT

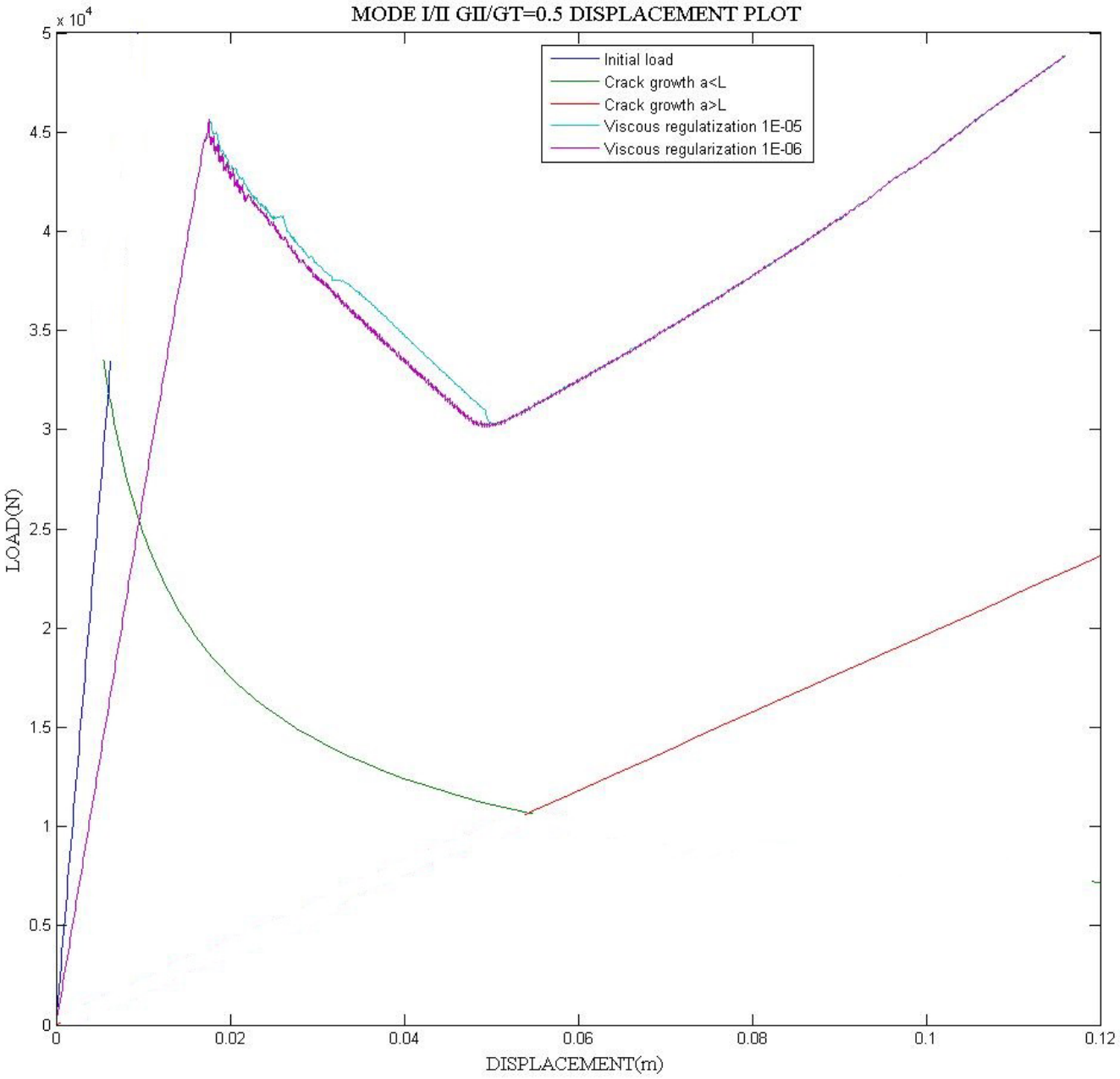

Fig. 35 Mode I/II X-FEM COHESIVE SEGMENTS load/displacement plot

Figure 35 shows the load/displacement plot for X-FEMVCCT. As seen, the necessary load for initiate the crack from the analytical model is 32,019 N and from the numerically model the load obtained was 45,644 N, the difference is about 42% off from the analytical model. Further investigation is needed to decide if this percentage off comes from the numerical or analytical model

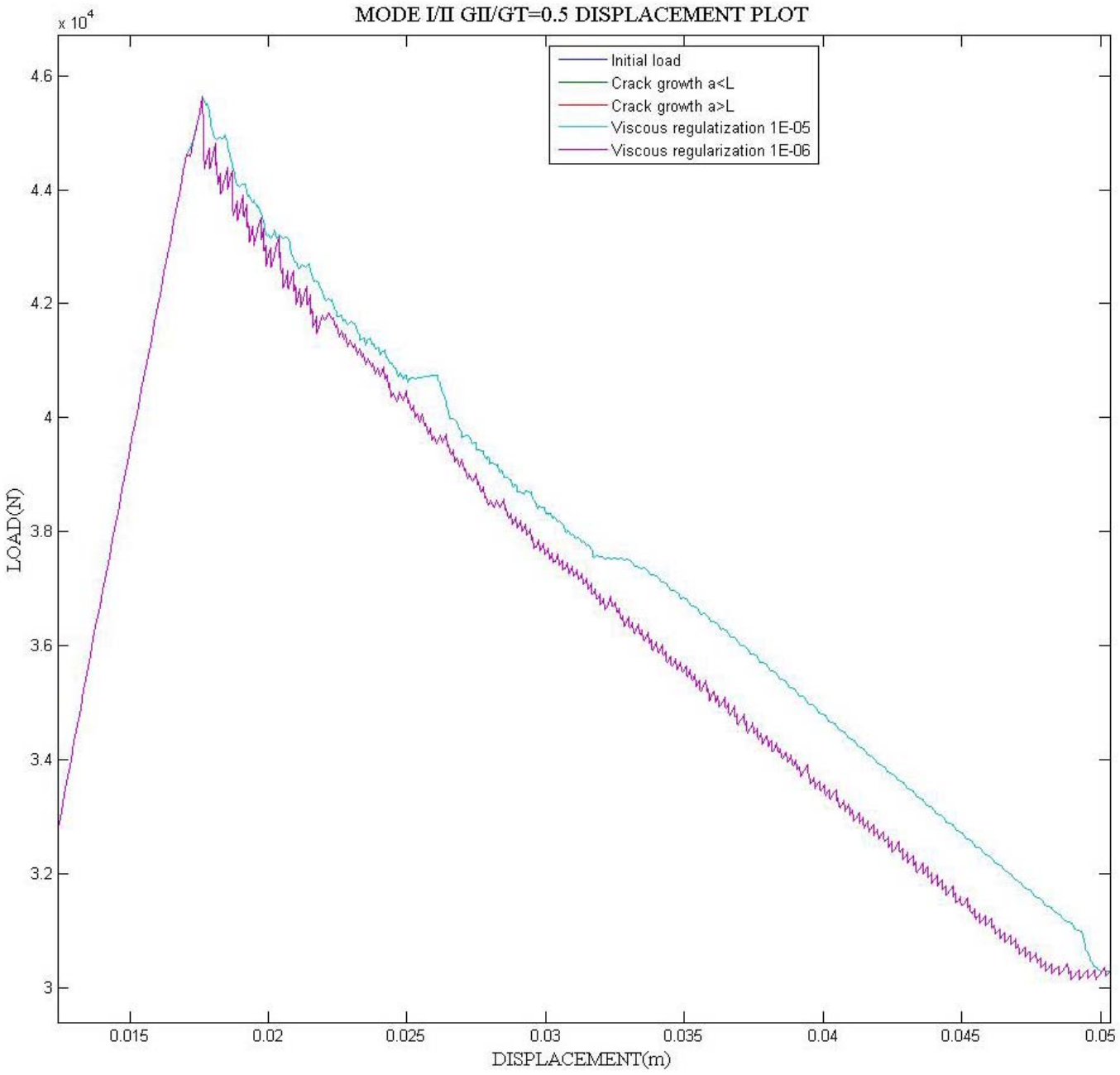

Fig. 36 Pattern difference using different viscosities for X-FEM VCCT

4.2.3 COMPARISON OF THE TWO TECHNIQUES

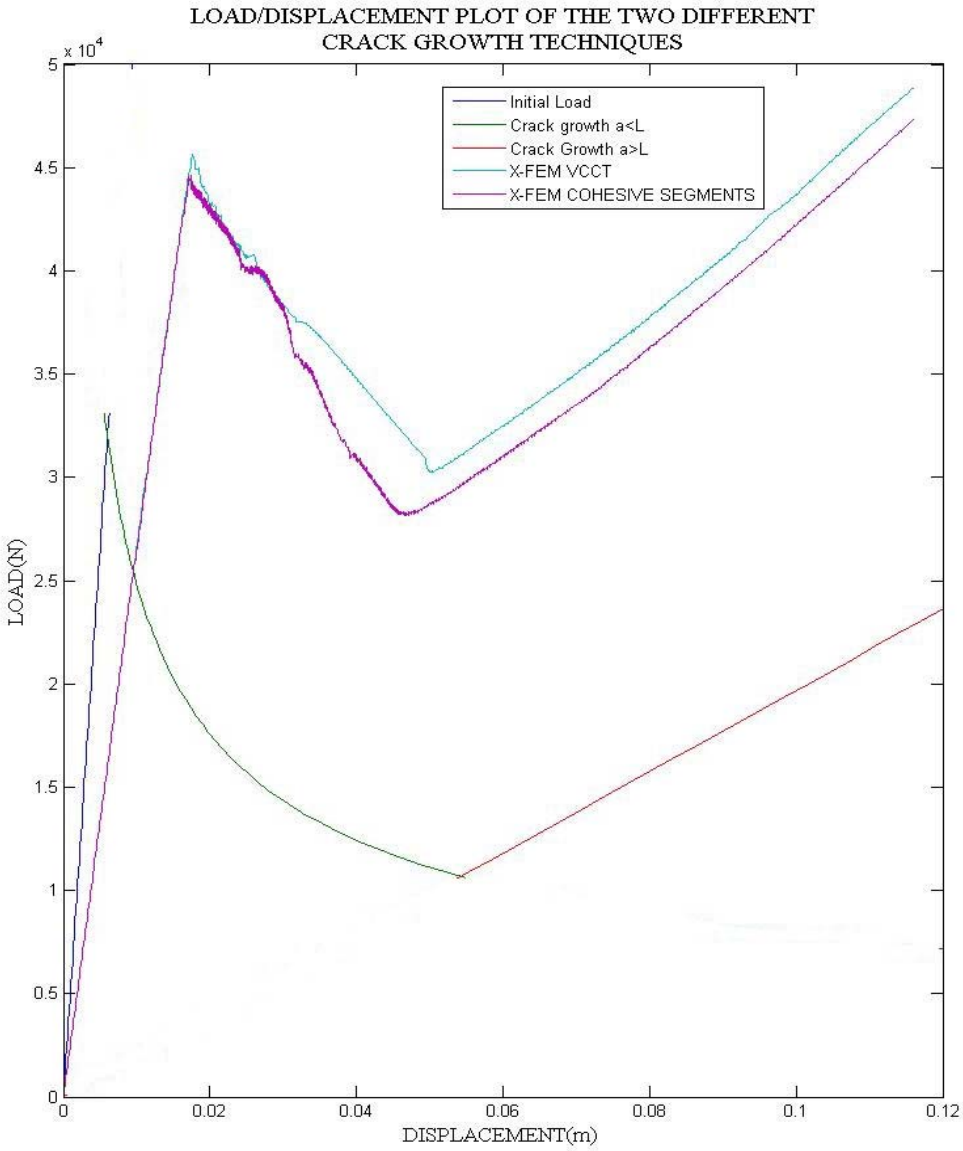

Fig. 37 Plot showing the two different techniques used.

The two techniques used are shown in figure 37, as in the previous study for mode I, X-FEM with cohesive segments needs a bigger load to star the crack based on the criterion used rather than X-FEM VCCT. For future work is needed to decrease the percentage off the model, options to accomplish this could be to use a quadratic power criterion, use BK criterion for fracture, and examine other option of beam theory.

4.3 J-INTEGRAL RESULTS

The results obtained from the contour analysis were close the analytical solution. Based on formula 5, the critical energy release rate for the specimen was $G_c = 12500\ \frac{J}{m^2}$. The results obtained from the analysis are presented in figure 38, 10 contours were chosen and the result obtained after the third contour is $J_C = 11241\ \frac{J}{m^2}$, which was the value used to compare against the analytical solution. This gives us an offset of 10% to the closed-form solution which is in good approximation. Figure 39 shows the opening of the crack once the remote stress is applied.

J - I N T E G R A L E S T I M A T E S

CRACK NAME	CRACKFRONT NODE SET	C O N T O U R S 1 2 3 4 5				
		6	7	8	9	10
H-OUTPUT-1_CRACK-1	-7-	1.1245E+04	1.1235E+04	1.1241E+04	1.1241E+04	1.1241E+04
		1.1241E+04	1.1242E+04	1.1241E+04	1.1241E+04	1.1241E+04

Fig. 38 Results from data file

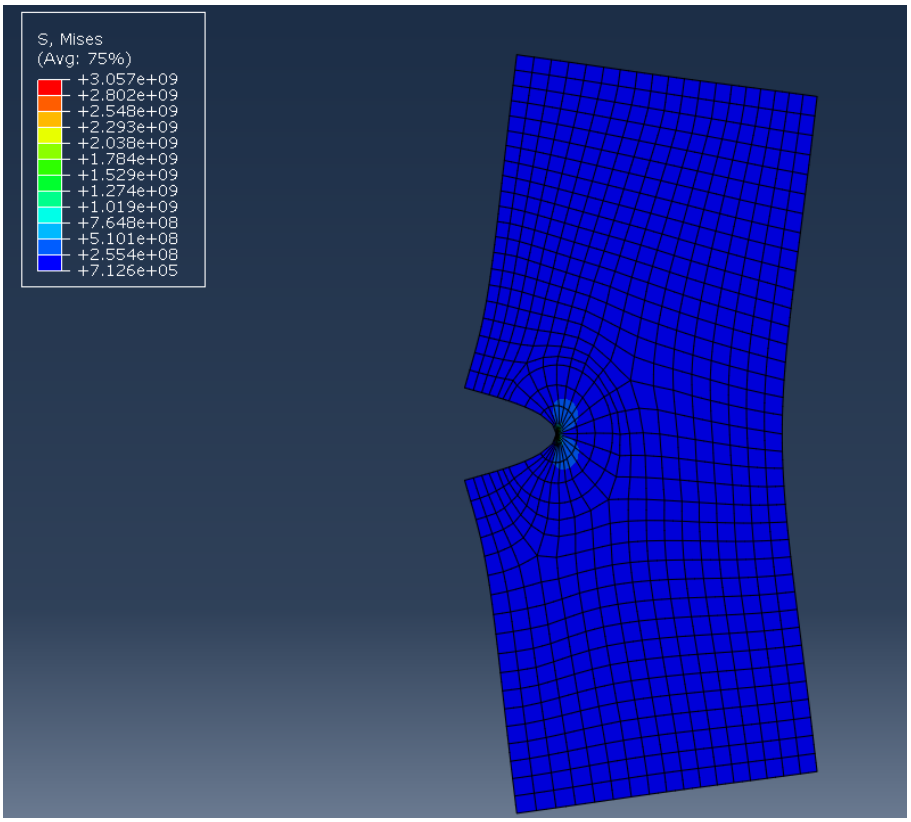

Fig. 39 Edge crack opening

5. CONCLUSION

In conclusion, ABAQUS capabilities for crack growth and calculation of energy release rate are accurate to certain degree against the closed-form analytical solutions as seen in the results section. The percentage off from the MMB is the one farther from the analytical solution. Crack growth in mode I and energy release rate analysis gave decent solution when compared to the analytical ones. As mentioned before, most of the work in crack growth analysis consisted in an iterative procedure, since converging was very difficult to obtain. It is important to mention that from all the techniques, implementing the routine of VCCT was the most difficult one. ABAQUS is not very user friendly at the moment of defining the master surface, slave surfaces, and the nodes of the slave surface, one have to go to the input file and create the node set and define the element edges for the surfaces manually. The energy release rate calculation challenge was to generate the mesh to create the singularity; defining the model parameters was straightforward. The techniques presented are a portion of the capabilities that ABAQUS has for fracture mechanics, but they are the foundation for more complex models.

6. RECOMMENDATIONS FOR FUTURE WORK

If a closed-form analytical approach is used to benchmark ABAQUS, some recommendations are given in order to assess ABAQUS further. For mode I propagation is recommended that the analytical model from introduced by Kanninen [10]. He recognized that simple beam theory did not properly model the interaction between the two arms of the DCB. The arms are not fixed against rotation at the crack tip; they rotate slightly due to the elastic support they provide one another. By using this analytical model, closer values to the ones obtained in the numerical model are expected. For mixed mode bending I/II, different ratios should be studied as well. A paper by Turon and Costa [18] gives a direct method to calculate c as the one used in this study. The ASTM standard for MMB testing [13] proposes to find c in an iterative solution procedure, Turon and Costa proposed the following formula to avoid the iterative procedure:

$$c = \frac{12\beta^2+3\alpha+8\beta\sqrt{3\alpha}}{36\beta^2-3\alpha} \tag{35}$$

Variables β and α are explained in detail in the paper.

Validation against experimental results is encouraged since analytical models sometimes cannot capture all the complexity of the fracture process.

REFERENCES

1. A.J. Kinloch, Y. Wang, J.G. Williams, P. Yayla, The mixed-mode delamination of fibre composite materials, Composites Science and Technology, Volume 47, Issue 3, 1993, Pages 225-237, ISSN 0266-3538
2. Abaqus Analysis User's Manual, ABAQUS® Standard, Version 6.11, DSS Simulia, 2011.
3. Anderson, Ted L. Fracture Mechanics: Fundamentals and Applications. Boca Raton: CRC Press, 1991. Print
4. ASTM D 6671-01, Standard Test Method for Mixed Mode I-Mode II Interlaminar Fracture Toughness of Unidirectional Fiber Reinforced Polymer Matrix Composites, in Annual Book of ASTM Standards, vol. 15.03: American Society for Testing and Materials, 2000
5. Belytschko, T., and T. Black, "Elastic Crack Growth in Finite Elements with Minimal Remeshing," International Journal for Numerical Methods in Engineering, vol. 45, pp. 601–620, 1999.Commercial Finite Element Codes," NASA/TM-2008-215123, 2008.
6. E 399-83, "Standard Test Method for Plane-Strain Fracture Toughness of Metallic Materials." American Society for Testing and Materials, Philadelphia, 1983.
7. E. F. Rybicki and M. F. Kanninen, A Finite Element Calculation of Stress Intensity Factors by a Modified Crack Closure Integral, Eng. Fracture Mech., Vol. 9, pp. 931-938, 1977.
8. Gdoutos, E. E. (2005). Fracture mechanics an introduction. Dordrecht, Springer.
9. Ingraffea A R. Computational Fracture Mechanics. Volume 2, Chapter 11, Encyclopedia of Computational Mechanics, E. Stein, R. de Borst, T. Hughes (eds.) John Wiley and Sons, 2004, 2nd Edition 2008.
10. Kanninen, M. F., "An Augmented Double Cantilever Beam Model for Studying Crack Propagation and Arrest," International Journal of Fracture, Vol.9, No.1, March 1973, pp.83-92.
11. Kregting, Rene, Cohesive Zone Models Toward a Robust Implementation of Irreversible Behavior. 2005
12. Mi, U., Crisfield, M.A., Davies, G.A.O., Progressive delamination using interface elements. Journal of Composite Materials, 32, 1246-1272, 1998.

13. N. Blanco, A. Turon, J. Costa, An exact solution for the determination of the mode mixture in the mixed-mode bending delamination test, Composites Science and Technology, Volume 66, Issue 10, August 2006, Pages 1256-1258, ISSN 0266-3538
14. R. Krueger, "An Approach to Assess Delamination Propagation Simulation Capabilities in
15. R. Krueger. Virtual Crack Closure Technique: History, Approach and Applications, Applied Mechanics Reviews, vol. 57, pp. 109-143, 2004.
16. Reeder JR, Crews Jr JH. Mixed-mode bending method for delamination testing. AIAA J 1990; 28(7):1270–6.
17. Rice, J.R.: A Path Independent Integral and the Approximate Analysis of Strain Concentration by Notches and Cracks, Journal of Applied Mechanics, 35 (1968), p. 379-386
18. Seong Hyeok Song, Glaucio H. Paulino, William G. Buttlar, A bilinear cohesive zone model tailored for fracture of asphalt concrete considering viscoelastic bulk material, Engineering Fracture Mechanics, Volume 73, Issue 18, December 2006, Pages 2829-2848, ISSN 0013-7944
19. Tenchev, RT & Falzon, BG 2007, 'A correction to the analytical solution of the mixed-mode bending (MMB) problem' Composites Science and Technology, vol 67, no. 3-4, pp. 662-668.
20. Wu, E. M., and R. C. Reuter Jr., “Crack Extension in Fiberglass Reinforced Plastics,” T and M Report, University of Illinois, vol. 275, 1965.

APPENDIX A. PARAMETERS FOR MMB

In[7]:= "TENCHEV PAPER";

```
Clear[P]
Clear[ii]
Clear[c]
Clear[L]
```

$$G1 = \frac{P^2 * L^2}{B * ee * ii} * \left(\frac{1}{2}\left(\frac{c}{L} - 3\right)^2 \left(\frac{a}{L}\right)^2 + \frac{1}{2}\left(\frac{c}{L} + 1\right)\left(5\frac{c}{L} - 13\right)\frac{a}{L} + \left(\frac{c}{L} + 1\right)\left(\frac{c}{L} + 3\right)\right);$$

$$G2 = \frac{P^2 * L^2}{B * ee * ii} * \left(\frac{3}{8}\left(\frac{c}{L} + 1\right)^2 \left(\frac{a}{L}\right)^2 - \left(\frac{c}{L} + 1\right)\left(2\frac{c}{L} + 1\right)\frac{a}{L} + \frac{1}{2}\left(\frac{c}{L} + 1\right)\left(5\frac{c}{L} + 1\right)\right);$$

In[14]:= $\frac{G1}{G2}$

Out[14]= $$\frac{\left(1 + \frac{c}{L}\right)\left(3 + \frac{c}{L}\right) + \frac{a^2\left(-3 + \frac{c}{L}\right)^2}{2L^2} + \frac{a\left(1 + \frac{c}{L}\right)\left(-13 + \frac{5c}{L}\right)}{2L}}{\frac{1}{2}\left(1 + \frac{c}{L}\right)\left(1 + \frac{5c}{L}\right) + \frac{3a^2\left(1 + \frac{c}{L}\right)^2}{8L^2} - \frac{a\left(1 + \frac{c}{L}\right)\left(1 + \frac{2c}{L}\right)}{L}}$$

In[15]:=
```
a = .6;
L = .4;
```

$$\text{Solve}\left[1 == \frac{\left(1 + \frac{c}{L}\right)\left(3 + \frac{c}{L}\right) + \frac{a^2\left(-3 + \frac{c}{L}\right)^2}{2L^2} + \frac{a\left(1 + \frac{c}{L}\right)\left(-13 + \frac{5c}{L}\right)}{2L}}{\frac{1}{2}\left(1 + \frac{c}{L}\right)\left(1 + \frac{5c}{L}\right) + \frac{3a^2\left(1 + \frac{c}{L}\right)^2}{8L^2} - \frac{a\left(1 + \frac{c}{L}\right)\left(1 + \frac{2c}{L}\right)}{L}}, c\right]$$

Out[17]= {{c → 0.275331}, {c → 0.370997}}

```
"-------------------------------------------------------------------------------------------------------------------------------
  ------------------------------------------------------------------------------"

"Solve for P"
```

In[18]:=
```
B = .2;
c = .37099;
ee = 200 000 000 000;
ii = .00000005625;
Solve[
```

$$1 == \left(\frac{1}{20000} * \frac{P^2 * L^2}{B * ee * ii} * \left(\frac{1}{2}\left(\frac{c}{L} - 3\right)^2 \left(\frac{a}{L}\right)^2 + \frac{1}{2}\left(\frac{c}{L} + 1\right)\left(5\frac{c}{L} - 13\right)\frac{a}{L} + \left(\frac{c}{L} + 1\right)\left(\frac{c}{L} + 3\right)\right)\right) + \left(\frac{1}{20000} * \frac{P^2 * L^2}{B * ee * ii} * \left(\frac{3}{8}\left(\frac{c}{L} + 1\right)^2 \left(\frac{a}{L}\right)^2 - \left(\frac{c}{L} + 1\right)\left(2\frac{c}{L} + 1\right)\frac{a}{L} + \frac{1}{2}\left(\frac{c}{L} + 1\right)\left(5\frac{c}{L} + 1\right)\right)\right),$$

```
P]
```

Out[22]= {{P → -21184.8}, {P → 21184.8}}

"----------
----------";

"Find displacement 1"

In[32]:= PP = 21184.826696534692;

$$P11 = \left(\frac{c}{L}\right) * PP$$

$$d111 = \frac{PP}{ee * ii} * \frac{\left(a^3 + \left(3 * a^2 * L\right) - L^3\right) * (L + c) - \left(4 * a^3 * L\right)}{6 * L}$$

Out[33]= 19648.4

Out[34]= 0.0821172

In[35]:= "----------
----------"

"Displacement 2.KINLOCH APPENDIX"

L = 0.4;

h = .015;

a = .6;

$$i = \frac{2 * B * h^3}{3};$$

$$BB = \frac{PP * a^3}{3 * ee * i} * \left(\frac{c}{L} - 7 * \left(1 - \frac{c + L}{2\,L}\right)\right);$$

$$A = \frac{PP}{6 * ee * i * 2\,L} * \left(\left(\left(\frac{c + L}{L}\right) * (2\,L - L)^3 - \left(1 - \frac{c + L}{2\,L} + \frac{c}{L}\right) * \left(2\,L^3\right)\right) - \frac{BB}{2\,L}\right);$$

$$D2222 = -\frac{PP * L^3}{6 * ee * i} * \left(1 - \frac{c + L}{2\,L} + \frac{c}{L}\right) - A * L - BB$$

Out[35]= ----------

Out[36]= Displacement 2.KINLOCH APPENDIX

Out[43]= -0.0081281

APPENDIX B. MODE I VCCT ROUTINE

```
**-----------------------------INTERACTIONS-----------------------------------------------------
*Initial Conditions, Type= Contact
 SLAVE, MASTER, NODE SLAVE
*Surface Interaction, name=IntProp-1
0.2
*Contact Pair, interaction=IntProp-1
SLAVE, MASTER
** ----------------------------------------------------------------
** ----------------------------------------------------------------
**
** STEP: CONTROLLED DISPLACEMENT
**
*Step, name="CONTROLLED DISPLACEMENT", inc=2000
*Static
0.001, 1., 1e-20, 0.001
**-----------------FRACTURE CRITERIA-------------------------
**-----------------------------------------------------------
*Debond, Slave=slave, Master=master, DEBONDING FORCE=RAMP
*Fracture Criterion, TOLERANCE=0.2, Type=VCCT, MIXED MODE BEHAVIOR=POWER, Viscosity=.000001
20000.0, 0.0, 0.0, 1.0, 1.0, 1.0
**-----------------------------------------------------
**
** BOUNDARY CONDITIONS
**
** Name: U1 NEGATIVE Type: Displacement/Rotation
*Boundary
_PickedSet8, 1, 1
_PickedSet8, 2, 2, -0.049
** Name: U1 POSITIVE Type: Displacement/Rotation
*Boundary
_PickedSet7, 1, 1
_PickedSet7, 2, 2, 0.049
**
** OUTPUT REQUESTS
**
*Restart, write, frequency=0
**
** FIELD OUTPUT: F-Output-1
**
*contact print, Master=master, Slave=slave
OPENBC, EFENRRTR, BDSTAT
*Output, field, variable=PRESELECT
*contact output, Master=master, Slave=slave
OPENBC, EFENRRTR
```

APPENDIX C. MODE I XFEM-VCCT ROUTINE

```
*Enrichment, name="XFEM CRACK", type=PROPAGATION CRACK, elset=_PickedSet7, interaction=VCCT
*End Assembly
**
** MATERIALS
**
*Material, name="MMETAL ELASTIC XFEM"
*Elastic
 2e+11, 0.3
**
** INTERACTION PROPERTIES
**
*Surface Interaction, name=VCCT
0.2,
*Surface Behavior
*Fracture Criterion, tolerance=0.5, type=VCCT, mixed mode behavior=Power, normal direction=2, viscosity=1e-08
20000.,0.0, 0.0, 1.0, 1.0, 1.0
*Initial Conditions, type=ENRICHMENT
```

APPENDIX D. MODE I XFEM-COHESIVE SEGMENTS ROUTINE

```
*Enrichment, name="XFEM COHESIVE", type=PROPAGATION CRACK, elset=_PickedSet7, interaction=GEOM
*End Assembly
**
** MATERIALS
**
*Material, name="METAL ELASTIC"
*Damage Initiation, criterion=MAXS, normal direction=2
 7.97815e+08,0.,0.
*Damage Evolution, type=ENERGY, mixed mode behavior=POWER LAW, power=1.
20000.,20000.,    0.
*Damage Stabilization
1e-06
*Elastic
 2e+11, 0.3
**
** INTERACTION PROPERTIES
**
*Surface Interaction, name=GEOM
0.2,
```

APPENDIX E. MIXED MODE I/II XFEM-VCCT ROUTINE

```
,
*Enrichment, name=Crack-1 XFEM, type=PROPAGATION CRACK, elset=_PickedSet7, interaction=VCCT
*End Assembly
**
** MATERIALS
**
*Material, name="METAL ELASTIC"
*Elastic
 2e+11, 0.3
**
** INTERACTION PROPERTIES
**
*Surface Interaction, name=VCCT
0.2,
*Surface Behavior
*Fracture Criterion, type=VCCT, mixed mode behavior=POWER, normal direction=2, viscosity=1e-07
20000.,20000.,20000000000000000.,    1.,    1.,    1.
```

APPENDIX F. MIXED MODE I/II XFEM-COHESIVE SEGMENTS ROUTINE

```
*,
*Enrichment, name="XFEM COHESIVE", type=PROPAGATION CRACK, elset=_PickedSet7, interaction=GEOM
*End Assembly
**
** MATERIALS
**
*Material, name="METAL ELASTIC"
*Damage Initiation, criterion=MAXS, normal direction=2
 7.97815e+08,0.,0.
*Damage Evolution, type=ENERGY, mixed mode behavior=POWER LAW, power=1.
20000.,20000.,    0.
*Damage Stabilization
1e-06
*Elastic
 2e+11, 0.3
**
** INTERACTION PROPERTIES
**
*Surface Interaction, name=GEOM
0.2,
*Initial Conditions, type=ENRICHMENT
```

VITA

Luis A. Hernández was born in Chihuahua, Chihuahua, México. He enrolled at the University of Texas at El Paso in fall 2004 where he received his Bachelor of Science in Mechanical Engineering in 2009; afterwards he worked in the industry as a components engineer. In the spring of 2012 he decided to pursue his Master of Science degree in Mechanical Engineering at the University of Texas at El Paso. In summer 2013, he obtained his Master of Science degree.

Permanent address: 299 King's Point Dr
El Paso, TX 79912

This thesis/dissertation was typed by Luis A. Hernandez.